

## MIT Open Access Articles

### *Renaissance of the ~1 TeV fixed-target program*

The MIT Faculty has made this article openly available. **Please share** how this access benefits you. Your story matters.

**Citation:** Adams, T. et al. "Renaissance of the ~1 TeV fixed-target program." International Journal of Modern Physics A 25.4 (2010): 777-813.

**As Published:** <http://dx.doi.org/10.1142/S0217751X10047774>

**Publisher:** World Scientific Publishing

**Persistent URL:** <http://hdl.handle.net/1721.1/63183>

**Version:** Author's final manuscript: final author's manuscript post peer review, without publisher's formatting or copy editing

**Terms of use:** Creative Commons Attribution-Noncommercial-Share Alike 3.0



# Renaissance of the $\sim 1$ TeV Fixed-Target Program

T. Adams<sup>9</sup>, J. A. Appel<sup>7</sup>, K. E. Arms<sup>12</sup>, A. B. Balantekin<sup>21</sup>, J. M. Conrad<sup>10</sup>, P. S. Cooper<sup>7</sup>, Z. Djurcic<sup>6</sup>, W. Dunwoodie<sup>18</sup>, J. Engelfried<sup>3</sup>, P. H. Fisher<sup>10</sup>, E. Gottschalk<sup>7</sup>, A. de Gouvea<sup>14</sup>, K. Heller<sup>12</sup>, C. M. Ignarra<sup>10</sup>, G. Karagiorgi<sup>10</sup>, S. Kwan<sup>7</sup>, W. A. Loinaz<sup>1</sup>, B. Meadows<sup>5</sup>, R. Moore<sup>7</sup>, J. G. Morfin<sup>7</sup>, D. Naples<sup>16</sup>, P. Nienaber<sup>17</sup>, S. F. Pate<sup>13</sup>, V. Papavassiliou<sup>13</sup>, A. A. Petrov<sup>11,20</sup>, M. V. Purohit<sup>19</sup>, H. Ray<sup>8</sup>, J. Russ<sup>4</sup>, A. J. Schwartz<sup>5</sup>, W. G. Seligman<sup>6</sup>, M. H. Shaevitz<sup>6</sup>, H. Schellman<sup>14</sup>, J. Spitz<sup>\*,22</sup>, M. J. Syphers<sup>7</sup>, T. M. P. Tait<sup>2,14</sup>, and F. Vannucci<sup>15</sup>

<sup>1</sup>*Amherst College, Amherst, MA 01002*

<sup>2</sup>*Argonne National Laboratory, Argonne, IL 60439*

<sup>3</sup>*Universidad Autónoma de San Luis Potosí, Mexico 78240*

<sup>4</sup>*Carnegie-Mellon University, Pittsburgh, PA 15213*

<sup>5</sup>*University of Cincinnati, Cincinnati, OH 45221*

<sup>6</sup>*Columbia University, New York, NY 10027*

<sup>7</sup>*Fermi National Accelerator Laboratory, Batavia, IL 60510*

<sup>8</sup>*University of Florida, Gainesville, FL 32611*

<sup>9</sup>*Florida State University, Tallahassee, FL 32306*

<sup>10</sup>*Massachusetts Institute of Technology, Cambridge, MA 02139*

<sup>11</sup>*University of Michigan, Ann Arbor, MI 48201*

<sup>12</sup>*University of Minnesota, Minneapolis, MN 55455*

<sup>13</sup>*New Mexico State University, Las Cruces, NM 88003*

<sup>14</sup>*Northwestern University, Chicago, IL 60208*

<sup>15</sup>*University Paris 7, APC, Paris, France*

<sup>16</sup>*University of Pittsburgh, Pittsburgh, PA 15260*

<sup>17</sup>*Saint Mary's University of Minnesota, Winona, MN 55987*

<sup>18</sup>*SLAC National Accelerator Laboratory, Stanford, CA 94309*

<sup>19</sup>*University of South Carolina, Columbia, SC 29208*

<sup>20</sup>*Wayne State University, Detroit, MI 48201*

<sup>21</sup>*University of Wisconsin, Madison, WI 53706*

<sup>22</sup>*Yale University, New Haven, CT 06520*

December 27, 2010

## Abstract

This document describes the physics potential of a new fixed-target program based on a  $\sim 1$  TeV proton source. Two proton sources are potentially available in the future: the existing Tevatron at Fermilab, which can provide 800 GeV protons for fixed-target physics, and a possible upgrade to the SPS at CERN, called SPS+, which would produce 1 TeV protons on target. In this paper we

---

\*Corresponding author

Email address: [joshua.spitz@yale.edu](mailto:joshua.spitz@yale.edu) (J. Spitz)

use an example Tevatron fixed-target program to illustrate the high discovery potential possible in the charm and neutrino sectors. We highlight examples which are either unique to the program or difficult to accomplish at other venues.

## 1 Introduction

*Fixed-target at approximately TeV energies? Didn't we do that for over twenty years ending a decade ago? Why revisit that strategy?*

A renaissance in TeV-energy fixed-target physics has become possible because of new detector technologies and improvements in accelerators since the 1990's. As a result, we can describe a fixed-target physics program, focusing on the charm and neutrino sectors. The program is unique to a  $\sim 1$  TeV fixed-target facility and complements the ongoing physics program envisioned by the community for the late 2010's.

There are two possible sources of  $\sim 1$  TeV protons which may be available. The first is the Tevatron at Fermilab, which can be modified for fixed-target running. Details on how this machine can be run at higher intensity and higher efficiency than in the past are discussed in Appendix A of this paper. The second possible source is the SPS+ [1, 2] which is planned at CERN as part of the LHC upgrade program. The fixed-target program described here can run during times when the SPS+ is not providing beam to LHC. The energy of SPS+ is expected to be about 1 TeV. For the results presented here, we have assumed 800 GeV protons on target since this is the capability of the existing machine. However, the physics case only improves for running at 1 TeV.

The purpose of this paper is to illustrate the strength and richness of an envisioned fixed-target program. In particular, this paper concentrates on a new study of discovery potential in the charm sector, which would utilize slow-spill beams. A future  $D^0$ - $\bar{D}^0$  mixing and  $CP$  violation ( $CPV$ ) experiment with three years of running could reconstruct an order of magnitude more flavor-tagged  $D^0 \rightarrow K^+ \pi^-$  decays than will be reconstructed by the  $B$ -factory experiments with their full data sets. The resulting sensitivity to  $CPV$  parameters  $|q/p|$  and  $\text{Arg}(q/p)$  is found to be much greater than current world sensitivity. However, to illustrate that this is a well-rounded program, we also explore ideas in the neutrino sector. We review the case for a precision electroweak neutrino experiment running from a very pure sign-selected high energy  $\nu_\mu$  beam, which has been discussed in more detail elsewhere [3, 4] and we present new studies on two promising and unique avenues for beyond Standard Model neutrino searches using beam dump production. The first of these uses  $\nu_\tau$  charged current events produced by a proton beam in the 800 GeV to 1 TeV range. The second is a search for neutral heavy leptons produced in the beam dump. Emphasizing the breadth of physics possible in the high-energy neutrino scattering sector of this new fixed target program, an extensive study of high-precision QCD is described in a separate paper [4].

This combination of experiments represents an integrated program aimed at discovery of new physics. At the same time, each of these experiments will provide a wide array of interesting and valuable measurements within the Standard Model. The program is very physics rich and will provide opportunities for many physicists. The result is a compelling opportunity for the future.

## 2 The Discovery Potential of Fixed-Target Charm

### 2.1 Introduction

As mentioned, there was a very successful fixed-target charm program at the Fermilab Tevatron [5]. Not only did it provide high precision measurements (some of which remain the most precise even today), but it also advanced flavor physics thinking in a way that still underlies many current analyses. It also demonstrated the utility of precision vertexing for heavy flavor physics, paving the way for

the incorporation of silicon tracking systems in all the latest experiments. The fixed-target charm program ended when the applied technologies were more-or-less played out, and attention turned to the opportunities at colliders, both at  $e^+e^-$  and hadron machines. The reason to now revisit the possibility of a fixed-target charm experiment is a combination of increased interest in charm mixing (now observed) and possible  $CPV$  in the charm system, and the availability of technology well beyond what was available at the end of the previous program [6, 7, 8, 9, 10, 11, 12, 13, 14]. A Tevatron fixed-target experiment may be the most cost-effective way forward in the charm sector, as the Tevatron would not need to be run in collider mode. Also, the beam energy could be reduced and still remain far above charm production threshold. Such an experiment at the Tevatron has the potential to greatly improve upon the sensitivity to mixing and  $CPV$  achieved by the B factories. We note that the most sensitive measurements of mixing and  $CPV$  rely on measuring decay-time distributions. For this type of measurement, a fixed-target experiment has an advantage over an  $e^+e^-$  B factory experiment due to the fact that the mean decay length is notably larger than the vertex resolution. We will address these physics opportunities below. In the recent “Roadmap for US High-Energy Physics” written by the Particle Physics Project Prioritization Panel (P5), future operation of the Tevatron was not considered. However, there exists a plan to keep the Tevatron cold after completion of the collider program such that it could easily be operated again should sufficiently compelling physics opportunities arise.

A Fermilab Tevatron fixed-target experiment could produce very large samples of  $D^*$  mesons that decay via  $D^{*+} \rightarrow D^0\pi^+$ ,  $D^0 \rightarrow K^+\pi^-$ <sup>1</sup>. The decay time distribution of the “wrong-sign”  $D^0 \rightarrow K^+\pi^-$  decay is sensitive to  $D^0$ - $\bar{D}^0$  mixing parameters  $x$  and  $y$ . Additionally, comparing the  $D^0$  decay time distribution to that for  $\bar{D}^0$  allows one to measure or constrain the  $CPV$  parameters  $|q/p|$  and  $\text{Arg}(q/p) \equiv \phi$ . This method has been used previously by Fermilab experiments E791 [15] and E831 [16] to search for  $D^0$ - $\bar{D}^0$  mixing. However, those experiments ran in the 1990’s and reconstructed only a few hundred flavor-tagged  $D^0 \rightarrow K^+\pi^-$  decays. Technological advances in vertexing detectors and electronics made since then make a much improved fixed-target experiment possible. We estimate the expected sensitivity of such an experiment, and compare it to that of the B factory experiments Belle and BaBar. Those experiments have reconstructed several thousand signal decays and using these samples, along with those for  $D^0 \rightarrow K^+K^-/\pi^+\pi^-$ , have made the first observation of  $D^0$ - $\bar{D}^0$  mixing [17, 18]. The CDF experiment has also measured  $D^0$ - $\bar{D}^0$  mixing using  $D^0 \rightarrow K^+\pi^-$  decays [19]. Although the background is much higher than at an  $e^+e^-$  experiment, the number of reconstructed signal decays is larger, and the statistical errors on the mixing parameters are similar to those of BaBar.

Although we focus on measuring  $x$ ,  $y$ ,  $|q/p|$ , and  $\phi$ , a much broader charm physics program is possible at a Tevatron experiment. We also briefly present some of these other opportunities.

## 2.2 Expected signal yield

We estimate the expected signal yield by scaling from two previous fixed-target experiments, E791 at Fermilab and *HERA-B* at DESY. These experiments had center-of-mass energies and detector geometries similar to those that a new charm experiment at the Tevatron would have.

### 2.2.1 Scaling from *HERA-B*

*HERA-B* took data with various trigger configurations. One configuration used a minimum-bias trigger, and from this data set the experiment reconstructed  $61.3 \pm 13$   $D^*$ -tagged “right-sign”  $D^0 \rightarrow K^-\pi^+$

---

<sup>1</sup>Charge-conjugate modes are implicitly included unless noted otherwise.

decays in  $182 \times 10^6$  hadronic interactions [20]. This yield was obtained after all selection requirements were applied. Multiplying this rate by the ratio of doubly-Cabibbo-suppressed to Cabibbo-favored decays  $R_D \equiv \Gamma(D^0 \rightarrow K^+\pi^-)/\Gamma(D^0 \rightarrow K^-\pi^+) = 0.380\%$  [21] gives a rate of reconstructed, tagged  $D^0 \rightarrow K^+\pi^-$  decays per hadronic interaction of  $1.3 \times 10^{-9}$ . To estimate the sample size a Tevatron experiment would reconstruct, we assume the experiment could achieve a similar fractional rate. If the experiment ran at an interaction rate of 7 MHz (which was achieved by *HERA-B* using a two-track trigger configuration), and took data for  $1.4 \times 10^7$  live seconds per year, then it would nominally reconstruct  $(7 \text{ MHz})(1.4 \times 10^7)(1.3 \times 10^{-9})(0.5) = 64000$  flavor-tagged  $D^0 \rightarrow K^+\pi^-$  decays per year, or 192000 decays in three years of running. Here we have assumed a trigger efficiency of 50% relative to that of *HERA-B*, which is a simple estimate: the trigger needs to be more restrictive than the minimum-bias configuration of *HERA-B*, but, on the other hand, the technology has advanced since *HERA-B* was designed and the trigger latency and other inefficiencies should be substantially reduced.

### 2.2.2 Scaling from E791

Fermilab E791 was a charm hadroproduction experiment that took data during the 1991-1992 fixed-target run. The experiment ran with a modest transverse-energy threshold trigger, and it reconstructed 35  $D^*$ -tagged  $D^0 \rightarrow K^+\pi^-$  decays in  $5 \times 10^{10}$  hadronic interactions [15]. This corresponds to a rate of  $7 \times 10^{-10}$  reconstructed decays per hadronic interaction. Assuming a future Tevatron experiment achieves this fractional rate, one estimates a signal yield of  $(7 \text{ MHz})(1.4 \times 10^7)(7 \times 10^{-10}) = 69000$  per year, or 207000 in three years. This value is similar to that obtained by scaling from *HERA-B*. We have assumed the same trigger + reconstruction efficiency as that of E791. We note that E791 had an inactive region in the middle of the tracking stations where the  $\pi^-$  beam passed through, and a future Tevatron experiment could avoid this acceptance loss. We do not include any improvement for this in our projection.

### 2.3 Comparison with the $B$ factories

We compare these yields with those that will be attained by the  $B$  factory experiments after they have analyzed all their data. The Belle experiment reconstructed 4024  $D^*$ -tagged  $D^0 \rightarrow K^+\pi^-$  decays in  $400 \text{ fb}^{-1}$  of data [22], and it is expected to record a total of  $1000 \text{ fb}^{-1}$  when it completes running. This integrated luminosity corresponds to 10060 signal events.

The BaBar experiment reconstructed 4030 tagged  $D^0 \rightarrow K^+\pi^-$  decays in  $384 \text{ fb}^{-1}$  of data [17], and the experiment recorded a total of  $484 \text{ fb}^{-1}$  when it completed running in early 2008. Thus the total BaBar data set corresponds to 5080 signal events. Adding this to the estimated final yield from Belle gives a total of 15100  $D^0 \rightarrow K^+\pi^-$  decays. This is less than 8% of the yield estimated for a Tevatron experiment in three years of running.

The KEK-B accelerator where Belle runs is scheduled to be upgraded to a “Super- $B$ ” factory running at a luminosity of  $\sim 8 \times 10^{35} \text{ cm}^{-2} \text{ s}^{-1}$  [23]. There is also a proposal to construct a Super- $B$  factory in Italy near the I.N.F.N. Frascati laboratory [24]. An experiment at either of these facilities would reconstruct very large samples of  $D^{*+} \rightarrow D^0\pi^+$ ,  $D^0 \rightarrow K^+\pi^-$  decays. In fact the resulting sensitivity to  $x'^2$  and  $y'$  may be dominated by systematic uncertainties. This merits further study. We note that many of the systematic errors obtained at a future Tevatron experiment are expected to be smaller than those at an  $e^+e^-$  collider experiment, due to the superior vertex resolution and  $\pi/K$  identification possible with a forward-geometry detector.

### 2.4 Comparison with hadron colliders

The LHCb experiment has a forward geometry and is expected to reconstruct  $D^{*+} \rightarrow D^0\pi^+$ ,  $D^0 \rightarrow K^+\pi^-$  decays in which the  $D^*$  originates from a  $B$  decay. The resulting sensitivity to mixing param-

eters  $x'^2$  and  $y'$  has been studied in Ref. [25]. This study assumes a  $b\bar{b}$  cross section of  $500 \mu\text{b}$  and estimates several unknown trigger and reconstruction efficiencies. It concludes that approximately 58000 signal decays would be reconstructed in  $2 \text{ fb}^{-1}$  of data, which corresponds to one year of running. This yield is similar to that estimated for a Tevatron experiment. However, LHCb's trigger is efficient only for  $D$  mesons having high  $p_T$ , *i.e.* those produced from  $B$  decays. This introduces two complications:

1. Some fraction of prompt  $\bar{D}^0 \rightarrow K^+\pi^-$  decays will be mis-reconstructed or undergo multiple scattering and, after being paired with a random soft pion, will end up in the  $D^0 \rightarrow K^+\pi^-$  sample (fitted for  $x'^2$  and  $y'$ ). As the production rate of prompt  $D$ 's is two orders of magnitude larger than that of  $B$ 's, this component may be non-negligible, and thus would need to be well-understood when fitting.
2. To obtain the  $D^*$  vertex position (*i.e.* the origin point of the  $D^0$ ), the experiment must reconstruct a  $B \rightarrow D^*X$  vertex, and the efficiency for this is not known. Monte Carlo studies indicate it is 51% [25], but there is uncertainty in this value.

The LHCb study found that, for  $N_{K^+\pi^-} = 232500$ , a signal-to-background ratio ( $S/B$ ) of 0.40, and a decay time resolution ( $\sigma_t$ ) of 75 fs, the statistical errors obtained for  $x'^2$  and  $y'$  were  $6.4 \times 10^{-5}$  and  $0.87 \times 10^{-3}$ , respectively. These values are less than half of those that we estimate can be attained by the  $B$  factories by scaling current errors by  $\sqrt{N_{K^+\pi^-}}$ :  $\delta x'^2 \approx 14 \times 10^{-5}$  and  $\delta y' \approx 2.2 \times 10^{-3}$ . As the signal yield,  $S/B$ , and  $\sigma_t$  of a future Tevatron experiment are similar to those for LHCb, we expect that similar errors for  $x'^2$  and  $y'$  can be attained.

The CDF measurement of charm mixing [19] uses 12700  $D^{*+} \rightarrow D^0\pi^+$ ,  $D^0 \rightarrow K^+\pi^-$  decays from  $1.5 \text{ fb}^{-1}$  of integrated luminosity. This could increase by about a factor of five by the end of Run II at the Tevatron collider. Assuming that both statistical and systematic errors are reduced by the square root of the anticipated increase in luminosity, one estimates errors of  $16 \times 10^{-5}$  and  $3.4 \times 10^{-3}$  for  $\delta x'^2$  and  $\delta y'$ , respectively, at the end of Run II.

To compare to these estimates, we have done a ‘‘toy’’ Monte Carlo (MC) study to estimate the sensitivity of a Tevatron experiment. The results obtained are similar to those of LHCb: for  $N_{K^+\pi^-} = 200000$ ,  $S/B = 0.40$ ,  $\sigma_t = 75 \text{ fs}$ , and a minimum decay time cut of  $0.5 \times \tau_D$  (to reduce combinatorial background), we find  $\delta x'^2 = 5.8 \times 10^{-5}$  and  $\delta y' = 1.0 \times 10^{-3}$ . These errors are the RMS's of the distributions of residuals obtained from fitting an ensemble of 200 experiments. A typical fit is shown in Fig. 1.

Note that it is difficult to know when a Tevatron charm experiment might be performed and results available. That makes it challenging to say what may be the world situation by the time such an experiment is done. The point of this paper is to say what such an experiment might achieve.

## 2.5 Global fit for $CPV$ parameters

If we assume the  $\delta x'^2$  and  $\delta y'$  errors obtained in our toy MC study (which are close to the values obtained in the LHCb study), we can estimate the resulting sensitivity to  $CPV$  parameters  $|q/p|$  and  $\phi$ . The first parameter characterizes  $CPV$  in the mixing of  $D^0$  and  $\bar{D}^0$  mesons, while the second parameter is a phase that characterizes  $CPV$  resulting from interference between an amplitude with mixing and a direct decay amplitude. In the Standard Model,  $|q/p|$  and  $\phi$  are essentially 1 and 0, respectively. A measurable deviation from these values would indicate new physics.

To calculate the sensitivity to  $|q/p|$  and  $\phi$ , we do a global fit of eight underlying parameters to 28 measured observables. The fitted parameters are  $x$  and  $y$ , strong phases  $\delta_{K\pi}$  and  $\delta_{K\pi\pi}$ ,  $R_D$ , and  $CPV$  parameters  $A_D$ ,  $|q/p|$  and  $\phi$ . Our fit is analogous to that done by the Heavy Flavor Averaging Group (HFAG) [26]. The only difference is that we reduce the errors for  $x'^2$  and  $y'$  according to our toy MC

study, and we also reduce the error for  $y_{CP}$  by a similar fraction. This latter parameter is measured by fitting the decay time distribution of  $D^0 \rightarrow K^+ K^- / \pi^+ \pi^-$  decays, which would also be triggered on and reconstructed by a Tevatron charm experiment.

The results of the fit are plotted in Fig. 2 (right). The figure shows two-dimensional likelihood contours for  $|q/p|$  and  $\phi$ . For comparison, the analogous HFAG plot as presented at the EPS 2009 conference is shown in Fig. 2 (left). One sees that a future Tevatron experiment would yield a very substantial improvement. However, by the time a Tevatron experiment runs, could the world situation be different from that shown in the HFAG plot? Much of the constraining power in the plot is due to the measurement of  $x'$  and  $y'$  in  $D^0 \rightarrow K^+ \pi^-$  decays, and of  $y_{CP}$  in  $D^0 \rightarrow K^+ K^- / \pi^+ \pi^-$  decays. For these observables, the Belle/BaBar data sets used consist of 400/540  $\text{fb}^{-1}$  and 384/384  $\text{fb}^{-1}$ , respectively; these together comprise about 65% of the total data set. Significant constraining power is also due to measurements of  $x$ ,  $y$ ,  $|q/p|$ , and  $\phi$  in  $D^0 \rightarrow K_S^0 \pi^+ \pi^-$  decays, and of  $x''$ ,  $y''$  in  $D^0 \rightarrow K^+ \pi^- \pi^0$  decays; for these measurements only about 30-40% of the total data set has been used. Thus we conclude that, once all Belle and Babar data is analyzed, the errors on the observables will improve by perhaps a factor of  $\sim \sqrt{2}$ . This is much less than the factor of 3-4 improvement in these observables used to produce Fig. 2 (right). The addition of more CDF data and of BESIII data will also improve the HFAG plot, but the improvement on top of that due to Belle and Babar is expected to be modest.

## 2.6 Other physics

### 2.6.1 Direct $CPV$ searches

In addition to searching for  $CPV$  arising from  $D^0$ - $\bar{D}^0$  mixing, one can search for direct  $CPV$  *i.e.*  $CP$  violation occurring in the decay amplitudes themselves. To search for this, one uses  $D^+$  or tagged- $D^0$  decays and looks for an asymmetry between the  $D \rightarrow f$  and  $\bar{D} \rightarrow \bar{f}$  decay rates.

Tables 1-2 are from the HFAG [27] and list current measurements of numerous direct  $CPV$  decay modes. Modes with 2- and 3-body final states could potentially be triggered on in a fixed-target Tevatron experiment and thus could be studied. The sensitivity to many of these modes is likely to be substantially greater than that of the current generation of experiments.

### 2.6.2 Spectroscopy via Dalitz-plot analyses

A very high statistics charm experiment can hope to unravel many mysteries related to resonances in the 1-2 GeV region. This is because charm hadron masses are in the 2 GeV range and  $\pi\pi$ ,  $K\pi$  and  $KK$  resonances often dominate charm particle decays. Below we describe two categories of measurements that could be done at a Tevatron charm experiment. In addition, there is much to be learned from

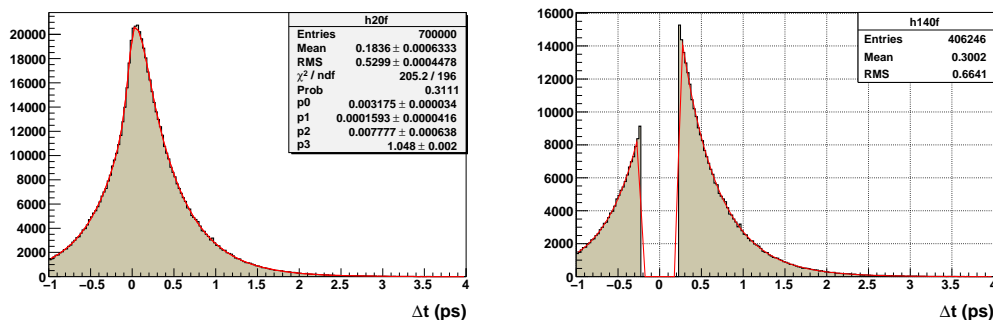


Figure 1: Monte Carlo  $D^0 \rightarrow K^+ \pi^-$  decay time distributions (left) without and (right) with a minimum decay time cut. Superimposed is the result of a fit. The ratio of signal to background after the  $t_{\min}$  ( $=\tau_D/2$ ) cut is 0.40, and the decay time resolution  $\sigma_t$  is 75 fs.

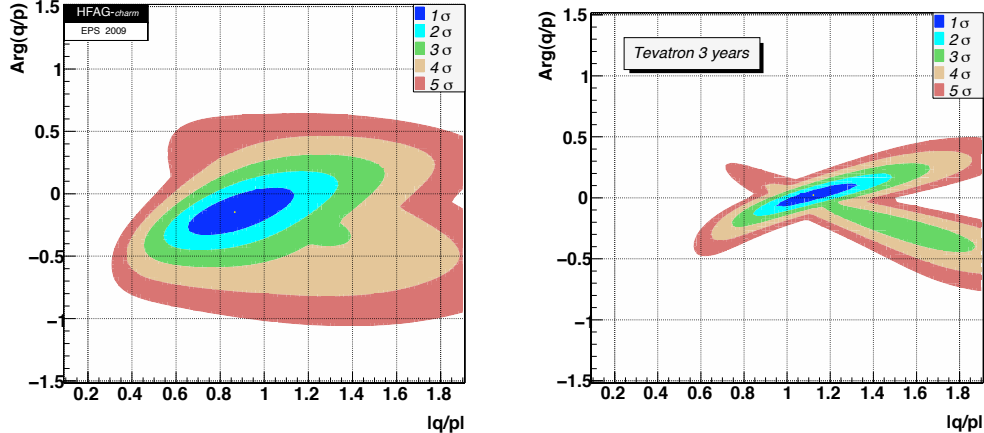


Figure 2:  $|q/p|$  versus  $\phi$  likelihood contours resulting from a global fit to measured observables (see text). Left: data after EPS 2009, from HFAG [26]. Right: after three years of running of a Tevatron charm experiment.

decays of the  $J/\psi$ ,  $\psi(2S)$ , and even the  $\eta_c$ , all of which would be copiously produced in a Tevatron charm experiment.

**Improvement in parameterizations of resonances** Thus far, experiments have used mainly a Breit-Wigner functional form to describe resonances, with some modifications for barrier penetration factors, etc. However, there is no well-established theory that prescribes a precise form for the propagator of wide resonances. Hence several deviations from simple forms have been proposed. For example, Gounaris and Sakurai [50] have proposed a formula for the case of the wide  $\rho(770)$  resonance. A well-known success is the Flatté formula [51] for a coupled-channel description of the  $f_0(980)$ . With regards to describing scalar resonances, both  $K$ -matrix and  $P$ -vector formalisms [52, 53, 54] have been proposed. The  $K$ -matrix method is attractive because it preserves unitarity, but the goodness-of-fit obtained is often no better than that obtained using a simple sum of resonances, and the  $K$  matrix itself contains implicit assumptions. Another issue is whether Zemach formalism [55] or helicity formalism [56, 57] correctly describes decays.

A scan of the particle data table of light, unflavored mesons shows that, beyond a mass of around  $1 \text{ GeV}/c^2$ , one or more of the mass, width, and major branching fractions of most resonances are not well-known. The parameters of the  $f_0(980)$  are not well-established. This is also true for strange mesons apart from the  $K^*(892)$ : the  $K_2^*(1430)$ ,  $K_3^*(1780)$ , and  $K_4^*(2045)$ . Other poorly measured or otherwise controversial states [58, 59] include the  $\sigma(600)$ ,  $\kappa(800)$ ,  $a_0(980)$ ,  $\eta(1295)$ ,  $\eta(1440)$ ,  $f_1(1420)$ , and  $f_1(1510)$ . A charm experiment at the Tevatron could clarify whether all these states exist and, if so, measure their parameters with much improved precision.

**Spectroscopy via production (e.g., double charm baryons)** Doubly-charmed baryons were discovered [60] at Fermilab in forward hadroproduction with baryon beams. Several states have been reported, each in several decay modes. However, there has not yet been an independent confirmation of these states. A future Tevatron charm experiment would be able to confirm and study these states with a much larger data set than that used previously.

Mode	Year	Collaboration	$A_{CP}$
$D^+ \rightarrow K_s^0 \pi^+$	2007	CLEOc [28]	$-0.006 \pm 0.010 \pm 0.003$
	2002	FOCUS [29]	$-0.016 \pm 0.015 \pm 0.009$
$D^+ \rightarrow K_s^0 K^+$	2002	FOCUS [29]	$+0.071 \pm 0.061 \pm 0.012$
$D^+ \rightarrow \pi^+ \pi^- \pi^+$	1997	E791 [30]	$-0.017 \pm 0.042$ (stat.)
$D^+ \rightarrow K^- \pi^+ \pi^+$	2007	CLEOc [28]	$-0.005 \pm 0.004 \pm 0.009$
$D^+ \rightarrow K_s^0 \pi^+ \pi^0$	2007	CLEO-c [28]	$+0.003 \pm 0.009 \pm 0.003$
$D^+ \rightarrow K^+ K^- \pi^+$	2008	CLEO-c [31]	$-0.0003 \pm 0.0084 \pm 0.0029$
	2007	CLEO-c [28]	$-0.001 \pm 0.015 \pm 0.008$
	2005	BABAR [32]	$+0.014 \pm 0.010 \pm 0.008$
	2000	FOCUS [33]	$+0.006 \pm 0.011 \pm 0.005$
	1997	E791 [30]	$-0.014 \pm 0.029$ (stat.)
	1994	E687 [34]	$-0.031 \pm 0.068$ (stat.)
$D^+ \rightarrow K^- \pi^+ \pi^+ \pi^0$	2007	CLEOc [28]	$+0.010 \pm 0.009 \pm 0.009$
$D^+ \rightarrow K_s^0 \pi^+ \pi^+ \pi^-$	2007	CLEOc [28]	$+0.001 \pm 0.011 \pm 0.006$
$D^+ \rightarrow K_s^0 K^+ \pi^+ \pi^-$	2005	FOCUS [35]	$-0.042 \pm 0.064 \pm 0.022$

Table 1:  $CP$  asymmetry  $A_{CP} = [\Gamma(D^+) - \Gamma(D^-)]/[\Gamma(D^+) + \Gamma(D^-)]$  for  $D^\pm$  decays.

## 2.7 Overview of new technologies

### 2.7.1 Silicon pixel detectors/vertexing

Silicon pixel detectors will play a crucial role in a new high-rate fixed-target charm experiment. Their contributions include pattern recognition in complex event topologies, radiation-hard high-rate capability so that the primary beam can go through the detector without compromising performance, and excellent spatial resolution enabling the reconstruction of interaction and decay points from measured charged particle tracks.

Historically, silicon microstrip detectors have played an important role in fixed-target charm experiments. When these high precision vertex detectors were introduced in the eighties, they revolutionized the study of heavy flavors. Besides offering high precision tracking and vertex information, they lead to the possibility of high statistics experiments, something that earlier generations of experiments, using bubble chambers or emulsions could not possibly accomplish. In 1985/1986, CCDs were used in a fixed-target charm experiment, the first application of pixel devices in high energy physics. Since then, silicon strip detectors have become major tracking elements in all collider experiments: for the Tevatron, LEP, B-factories, and now the LHC. CCDs were limited to only  $e^+e^-$  colliders because of their readout speed. On the other hand, hybridized pixel detectors, in which readout chips were bump-bonded to silicon sensors, have been used in heavy ion experiments at CERN (WA97, NA62) and are now being employed as the vertex detector for ATLAS, CMS, and ALICE. With the development and experience gained over the last decade or so, the hybridized pixel detector technology has matured, and certainly can be an important tool for future fixed-target charm experiments.

Pixel detectors offer excellent three-dimensional information, which leads to much better pattern recognition, avoiding ambiguities and ghost tracks. Its advantages over the two-dimensional information provided by the silicon strip detectors have been demonstrated by both the fixed-target experiments at CERN and also at SLD. With a pixel size of 50 microns by 400 microns, test beam results achieved a resolution of better than 2 microns. The detector noise is about 100 electrons or less. This means such a detector would give a signal-to-noise ratio of better than 200:1. These detectors are also very quiet, and the spurious hits, as observed during the commissioning phase of the LHC

Mode	Year	Collaboration	$A_{CP}$
$D^0 \rightarrow \pi^+\pi^-$	2008	Belle [36]	$+0.0043 \pm 0.0052 \pm 0.0012$
	2008	BABAR [37]	$-0.0024 \pm 0.0052 \pm 0.0022$
	2005	CDF [38]	$+0.010 \pm 0.013 \pm 0.006$
	2002	CLEO [39]	$+0.019 \pm 0.032 \pm 0.008$
	2000	FOCUS [33]	$+0.048 \pm 0.039 \pm 0.025$
	1998	E791 [40]	$-0.049 \pm 0.078 \pm 0.030$
$D^0 \rightarrow \pi^0\pi^0$	2001	CLEO [41]	$+0.001 \pm 0.048$ (stat. and syst. combined)
$D^0 \rightarrow K_s^0\pi^0$	2001	CLEO [41]	$+0.001 \pm 0.013$ (stat. and syst. combined)
$D^0 \rightarrow K^+K^-$	2008	Belle [36]	$-0.0043 \pm 0.0030 \pm 0.0011$
	2008	BABAR [37]	$+0.0000 \pm 0.0034 \pm 0.0013$
	2005	CDF [38]	$+0.020 \pm 0.012 \pm 0.006$
	2002	CLEO [39]	$+0.000 \pm 0.022 \pm 0.008$
	2000	FOCUS [33]	$-0.001 \pm 0.022 \pm 0.015$
	1998	E791 [40]	$-0.010 \pm 0.049 \pm 0.012$
	1995	CLEO [42]	$+0.080 \pm 0.061$ (stat.)
	1994	E687 [34]	$+0.024 \pm 0.084$ (stat.)
$D^0 \rightarrow K_s^0K_s^0$	2001	CLEO [41]	$-0.23 \pm 0.19$ (stat. and syst. combined)
$D^0 \rightarrow \pi^+\pi^-\pi^0$	2008	BABAR [43]	$-0.0031 \pm 0.0041 \pm 0.0017$
	2008	Belle [44]	$+0.0043 \pm 0.0130$
	2005	CLEO [45]	$+0.001^{+0.09}_{-0.07} \pm 0.05$
$D^0 \rightarrow K^+K^-\pi^0$	2008	BABAR [43]	$0.0100 \pm 0.0167 \pm 0.0025$
$D^0 \rightarrow K^-\pi^+\pi^0$	2007	CLEOc [28]	$+0.002 \pm 0.004 \pm 0.008$
	2001	CLEO [46]	$-0.031 \pm 0.086$ (stat.)
$D^0 \rightarrow K^+\pi^-\pi^0$	2005	BELLE [47]	$-0.006 \pm 0.053$ (stat.)
	2001	CLEO [48]	$+0.09^{+0.25}_{-0.22}$ (stat.)
$D^0 \rightarrow K_s^0\pi^+\pi^-$	2004	CLEO [49]	$-0.009 \pm 0.021^{+0.016}_{-0.057}$
$D^0 \rightarrow K^+\pi^-\pi^+\pi^-$	2005	BELLE [47]	$-0.018 \pm 0.044$ (stat.)
$D^0 \rightarrow K^+K^-\pi^+\pi^-$	2005	FOCUS [35]	$-0.082 \pm 0.056 \pm .047$

Table 2:  $CP$  asymmetry  $A_{CP} = [\Gamma(D^0) - \Gamma(\bar{D}^0)]/[\Gamma(D^0) + \Gamma(\bar{D}^0)]$  for  $D^0, \bar{D}^0$  decays.

experiments, are of order of  $10^{-5}$ . Furthermore, such devices can be self-triggered. All the readout chips used in the LHC experiments have the feature of being data-driven, which means that the chip generates a fast signal when a hit is registered above threshold. ALICE has used this information, and has taken a lot of cosmic ray and first beam data using a pixel-detector trigger.

Pixel detectors, because of their fine segmentation, can also handle very high rate, and handle high radiation dosage. These devices have all the excellent features that are required in a next generation of charm experiments.

Since 1998, Fermilab has been active in the pixel R&D effort. This has led to the development of the FPIX series of pixel readout chips for the BTeV experiment. When BTeV was cancelled, a group from Los Alamos picked up the design and used the chip, sensor, interconnect, and a lot of the mechanical design to build two forward muon stations for the PHENIX experiment. With small modifications, such a design could be well suited for a new charm experiment at the Tevatron.

### 2.7.2 Triggering on decay vertices, impact parameters

With the technical advances in detectors and electronics made since the last Fermilab fixed-target experiments, it is now possible to build a high-rate trigger system that selects charm events at the lowest trigger level by taking advantage of the key property that differentiates charm particles from other types of particles, namely their characteristic lifetimes. To achieve this, a new experiment would trigger on charm decay vertices by performing track and vertex reconstruction to search for evidence of a particle-decay vertex that is located tens to thousands of microns away from a primary interaction vertex. In practice, this would be done by reconstructing primary vertices and selecting events that have additional tracks with large impact parameters with respect to the primary vertex. The main advantage of this approach is that it suppresses light-quark background events while retaining high efficiency for charm events at the first stage of triggering by maximizing the trigger acceptance compared to trigger strategies that rely on detecting specific final-state particles, such as muons, or selecting events based on  $E_T$  cuts.

A trigger and data acquisition system for a new charm experiment would be able to take advantage of what has been learned from other experiments. While the power of silicon strip detectors for tracking and vertex reconstruction has been demonstrated by numerous experiments, it is the high-resolution three-dimensional tracking capability provided by a pixel vertex detector that permits a straightforward design for triggering on detached vertices at the first stage of a trigger system. A pixel vertex detector together with zero-suppressed readout of the data provide what is needed to perform the pattern recognition, track reconstruction, vertex reconstruction, and impact-parameter calculations that form the basis for a detached-vertex trigger. The design of the BTeV experiment's trigger was based on the following features:

- field programmable gate arrays (FPGAs) or comparable devices for pattern recognition;
- low-cost memory to buffer event data and allow for relatively long latencies in the first-level trigger;
- commodity off-the-shelf (COTS) networking and processing hardware.

BTeV demonstrated the possible tradeoffs between calculations performed by FPGAs and general-purpose processors. In the BTeV trigger FPGAs performed most of the pattern recognition for pixel data, since FPGAs excel at performing large numbers of rudimentary calculations in parallel. The remaining calculations were performed by general-purpose processors. One of the key features of the BTeV trigger was flexibility in the design that made it possible to move calculations performed in processors into FPGA hardware, thereby improving performance and reducing the cost of trigger hardware. Several FPGA-based algorithms were developed at Fermilab that could also be applied to a new charm experiment. Examples include an FPGA-based track segment finder and a fast “hash sorter” that sorted track-segment data before sending it to a general-purpose processor.

BTeV also demonstrated that advances in electronics make it possible to build a data acquisition system that will buffer event data long enough for a first-level trigger to analyze every interaction and perform complex operations to search for evidence of a detached vertex. The BTeV trigger design included enough memory to buffer data from the entire detector for approximately 800 ms, which was over three orders of magnitude more than the average processing time required by the first-level trigger. In addition to the large event buffer, the BTeV design relied on commodity networking and processing hardware to implement a sophisticated detached-vertex trigger that could be built for a reasonable cost. The key features of this design are being considered by the LHCb Collaboration for their upgrade in the middle of the next decade.

The CDF experiment has been using a decay-vertex trigger at the second level [61] to record large samples of two-body  $B$  and  $D$  decays. This success demonstrates the feasibility and capability of a

heavy-flavor-decay trigger used in a hadroproduction environment.

### 2.7.3 RICH detectors, $\pi/K$ separation

The physics goals of a fixed-target charm experiment require good charged particle identification to observe various decay modes of interest. At the Tevatron fixed-target energies, one must be able to separate pions, kaons, and protons with high efficiency over a range of momentum from several GeV up to hundreds of GeV. This can be accomplished by using a Ring Imaging Cherenkov detector (RICH).

From the early days of the OMEGA experiment, over the years, RICH detectors have been built and operated in different environments. They were used in fixed-target experiments at Fermilab (*e.g.* E665, E706, E789, E781), in *HERA-B* at DESY, as well as in  $e^+e^-$  collider experiments (CLEO, DELPHI and SLD). Currently, a RICH detector is used in a hadron collider experiment (LHCb).

The detector performance and cost is determined, to a large extent, by the choice of the photo-detector. In the early days, experiments used gas detectors based on photo-ionizing gas such as TMAE or TEA. Operationally, this has not been easy. On the other hand, the new rounds of experiments tend to use commercial detectors such as PMT (SELEX), MAPMT (*HERA-B*) and HPD (*LHCb*) which offer stability, ease of operation, and maintenance at a moderate cost.

We can take the SELEX RICH as an example. The RICH vessel is 10.22 m long, 93 inches in diameter and filled with neon at atmospheric pressure. At the end of the vessel, an array of 16 hexagonal mirrors are mounted on a low-mass panel to form a sphere of 19.8 m in radius. Each mirror is 10 mm thick, made out of low-expansion glass. For the photo-detector, SELEX used 2848 0.5-inch photomultiplier tubes arranged in an array of  $89 \times 32$ . Over a running period of 15 months, detector operation was very stable. The ring radius resolution was measured to be 1.56 mm and, on average, 13.6 photons were observed for a  $\beta = 1$  particle.

### 2.7.4 Micropattern gaseous tracking detectors, *e.g.* MSGC, GEM, and Micromegas

Previous generations of fixed-target charm experiments typically used large area gaseous detectors (*e.g.* drift chambers or multiwire gaseous chambers) for charged-particle tracking purposes. In high rate environments, these detectors suffered from inefficiency. In extreme environments, like regions around the incident beam, there was a dead region. For example, in the charm E-791 experiment at Fermilab, there was a large drift-chamber inefficiency (“hole”) around the beam line which had to be constantly monitored and corrected in the Monte Carlo acceptance calculations. This also led to significant loss in the overall efficiency of the spectrometer.

Since the early 1990’s, there have been substantial advances in micropattern gaseous detectors. These include MSGC (multistrip gaseous chamber), GEM (gaseous electron multiplier), and Micromegas devices. Currently, the state-of-the-art is that chambers as large as  $40 \times 40$  cm<sup>2</sup> can be built using either GEMs or Micromegas. These type of detectors have been operated reliably in the last generation of high rate fixed-target experiments such as COMPASS.

In a future high-rate heavy-flavor experiment, one can build a set of Micromegas or GEM detectors near the beam region to handle the high rate. Outside this region, the more conventional drift chambers can be used. This will allow operation at high rates with large area coverage.

## 2.8 Summary

In summary, we note the following and conclude:

- $D^0\text{-}\bar{D}^0$  mixing is now established, and attention has turned to the question of whether there is *CPV* in this system.

- Technical advances in detectors and electronics made since the last Fermilab fixed-target experiments ran would make a new experiment much more sensitive to mixing and  $CPV$  effects. Silicon strips and pixels for vertexing are well-developed, and detached-vertex-based trigger concepts and prototypes exist (*e.g.* *HERA-B*, CDF, BTeV, LHCb).
- Such an experiment would have substantially better sensitivity to mixing and  $CPV$  than all Belle and BaBar data together will provide. The Tevatron data should have less background than LHCb data. Systematic uncertainties may also be less than those of any Super- $B$  Factory experiments and LHCb.
- The Tevatron and requisite beamlines are essentially available.
- Such an experiment could help untangle whatever signals for new physics appear at the Tevatron or LHC.

Recently, a working group has formed to study the physics potential of a charm experiment at the Tevatron in more detail. Information about this working group and its results can be obtained at <http://www.nevis.columbia.edu/twiki/bin/view/FutureTev/WebHome>.

In brief, we write this chapter to keep the possibility of a fixed-target charm experiment at the Tevatron a viable option for Fermilab (and the broader international HEP program), to be decided upon once there is a clearer picture of available funding, manpower, and feasibility of the current roadmap.

### 3 Neutrino-electron Scattering

Neutrino-electron scattering ( $\nu_\mu + e \rightarrow \nu_\mu + e$ ) is an ideal process to search for beyond the Standard Model physics at Terascale energies through precision electroweak measurements. The low cross section for this process demands a very high intensity beam. In order to reduce systematics and reach a cross-section precision better than 1%, this process can be normalized to its charged-current sister, “inverse muon decay” ( $\nu_\mu + e \rightarrow \nu_e + \mu$ ). The threshold for this interaction is 11 GeV. Therefore, the experiment requires a high energy neutrino flux, as can only be provided by a  $\sim 1$  TeV primary proton beam. Once a high-energy, high-intensity neutrino flux is established, a detector optimized for  $\nu - e$  scattering can also be used for precision structure function and QCD measurements and direct searches.

The physics reach of NuSOng for beyond the Standard Model physics is in the 1 to 7 TeV range, depending on the model. The sensitivity to new physics complements the LHC and brings unique new opportunities to the program. The full physics program is discussed in detail elsewhere [3, 4, 62]. In this paper, we present an experimental overview which illustrates the value of this endeavor.

#### 3.1 The beam

For this discussion, we will assume a NuSOng beam design which is the same as that used by the NuTeV experiment (see Fig. 3), which ran from 1993-1996 at Fermilab [63]. We will assume  $2 \times 10^{20}$  high energy (800 GeV to 1 TeV) protons impinge on a beryllium oxide target. The resulting mesons traverse a quadrupole-focused, sign-selected magnetic beamline, hence the design is called a “sign-selected quad triplet” or SSQT. NuSOng will run with  $1.5 \times 10^{20}$  protons on target in neutrino mode, and  $0.5 \times 10^{20}$  protons on target in antineutrino mode. The result is a beam of very “right sign” purity ( $> 98\%$ ) and low  $\nu_e$  contamination (2%). The  $\nu_e$  in the beam are due mainly to  $K^+$  decays which can be well-constrained by the  $K^+ \rightarrow \nu_\mu$  flux which populates the high energy range of the neutrino flux. The magnetic bend substantially reduces  $\nu_e$  from  $K_L$  decay which tend to go forward and will thus not be directed at the detector.

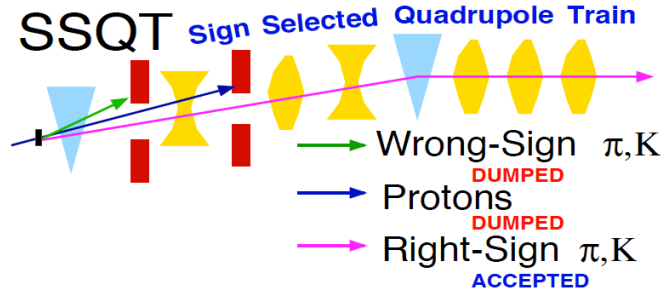


Figure 3: The NuSONG beam design, identical to that used by the NuTeV experiment. From Ref. [63].

### 3.2 The detector: segmented glass and LAr options

The baseline design for the NuSONG detector is a 3.5 kton glass-target design inspired by the design of the Charm II experiment. The detector is broken into four identical subdetectors, each consisting of a  $5\text{ m} \times 5\text{ m} \times 29\text{ m}$  target plus toroid muon spectrometer. Breaking the design into four sections assures high acceptance for muons produced in the target calorimeter to reach the toroid. A gap of 15 m extends between each detector to allow for a calibration beam to impinge on the target. The total length of the detector is, therefore, 200 m.

The total target is composed of 2500 sheets of glass which are 2.5 cm ( $0.25\lambda_0$ ) thick. This provides an isoscalar target for neutrino-quark interaction studies. Interspersed between the glass sheets are proportional tubes or scintillator planes. The total target mass is six times greater than NuTeV.

The signal processes are:  $\nu_\mu + e \rightarrow \nu_\mu + e$  and  $\nu_\mu + e \rightarrow \mu + \nu_e$ . These must be distinguished from the background processes of  $\nu_e + n \rightarrow e + p$  and  $\nu_\mu + n \rightarrow \mu + p$ . These processes become background for certain kinematic cases when the proton is not detected. In the initial studies for NuSONG, which was designed as interleaved one-radiation length glass targets and live detectors, a large systematic error came from the number of background events where the proton was lost in the glass [3]. Protons may be lost in the glass because they are produced at relatively wide angles and low energies. Motivated by this, the collaboration has been considering other designs for a target calorimeter.

LArTPC detectors provide a fully-live alternative in which the proton signature in background events is easily identified. Fig. 4 compares a 60 GeV  $\nu - e$  neutral current scatter in an LAr detector to a typical 60 GeV  $\nu_e + n$  background event. One can see that a proton track, which is at a large angle relative to the shower, is clearly visible. A 2 kton LArTPC detector is expected to have similar sensitivity to the 3.5 kton glass NuSONG detector. An LArTPC would require substantially less electronics than the glass detector, and should be proportionately less expensive.

The NuSONG LArTPC alternative is very similar in design to the technology for the  $\nu_\tau$  physics discussed later in this paper. The similarity between an LAr-based NuSONG and a future  $\nu_\tau$  detector is demonstrative of the synergy within this overall fixed-target program.

### 3.3 Neutral & charged current processes

Remarkable rates are acquired when the 3.5 kton detector is combined with the high intensity, high energy beam. One expects  $> 600\text{M}$   $\nu_\mu$  CC events and  $> 65\text{M}$   $\nu_e$  CC events. This can be compared to past samples of  $< 20\text{M}$  [64, 65, 66, 67, 68, 69, 70, 71, 72] and  $\sim 500\text{k}$  [64, 65, 66, 67, 68, 69, 70, 71, 72, 73, 74, 75, 76], respectively. With such large data samples, NuSONG can search for processes which

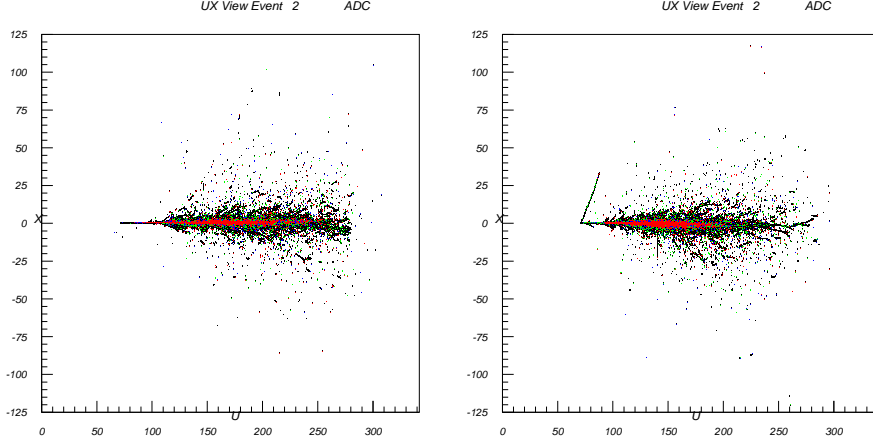


Figure 4: A 60 GeV  $\nu - e$  neutral current scatter in an LAr detector (left) and a typical 60 GeV  $\nu_e + n$  background event (right).

are within the Standard Model, but rare, or beyond the Standard Model which have not been studied before.

The expected rates for specific event types are given in Table 3. In particular, one should note that the  $\nu - e$  scattering sample is 40 times larger than that of previous experiments.

600M	$\nu_\mu$ CC Deep Inelastic Scattering
190M	$\nu_\mu$ NC Deep Inelastic Scattering
75k	$\nu_\mu$ electron NC elastic scatters (ES)
700k	$\nu_\mu$ electron CC quasi-elastic scatters (IMD)
33M	$\bar{\nu}_\mu$ CC Deep Inelastic Scattering
12M	$\bar{\nu}_\mu$ NC Deep Inelastic Scattering
7k	$\bar{\nu}_\mu$ electron NC elastic scatters (ES)
0k	$\bar{\nu}_\mu$ electron CC quasi-elastic scatters (WSIMD)

Table 3: Number of events in NuSOng assuming  $2 \times 10^{20}$  protons on target. NC indicates “neutral current” and CC indicates “charged current.”

The high event rates for neutrino neutral current scattering provide a remarkable opportunity to probe for new physics through the weak mixing angle,  $\sin^2 \theta_W$ , and the ratio of neutral to charged current couplings,  $\rho$ . This physics can be accessed through four modes:  $\nu_\mu + e^- \rightarrow \nu_\mu + e^-$ ,  $\bar{\nu}_\mu + e^- \rightarrow \bar{\nu}_\mu + e^-$ ,  $\nu_\mu + q \rightarrow \nu_\mu + q$ , and  $\bar{\nu}_\mu + q$ . There has been a long history of experiments which have exploited precision neutral current quark scattering, but the ultra-high rates for neutrino-electron scattering are a new opportunity raised by the high-energy, high-intensity primary beam. A deviation from the Standard Model predictions in both the electron and quark measurements would present a compelling case for new physics.

An essential feature to the NuSOng  $\nu - e$  study is that the NC event rate can be normalized to the CC process, called “inverse muon decay” (IMD),  $\nu_\mu + e^- \rightarrow \nu_e + \mu^-$ . This process is well understood in the Standard Model due to precision measurement of muon decay [77]. Since the data samples are collected with the same beam, target, and detector at the same time, the ratio of ES to IMD events cancels many systematic errors while maintaining a strong sensitivity to the physics of interest. Our measurement goal of the ES to IMD ratio is a 0.7% error, adding systematic and statistical errors in quadrature [3]. The high sensitivity which we propose arises from the combined high energy and high

intensity of the NuSOnG design, leading to event samples more than an order of magnitude larger than past experiments.

Normalizing the ES to the IMD events – which can only occur because of the TeV-scale primary beam – represents a crucial step forward from past ES measurements, which have normalized neutrino-mode ES measurements to antineutrino mode,  $\bar{\nu}_\mu + e^- \rightarrow \bar{\nu}_\mu + e^-$  [67, 78]. In fact, the level of precision expected from NuSOnG cannot be reached in lower energy experiments using antineutrino normalization. The improvement from the NuSOnG method is in both the experimental and the theoretical aspects of the measurement. First, the flux contributing to IMD and  $\nu$ ES is identical, whereas neutrino and antineutrino fluxes are never identical and so require corrections. Second, the ratio of  $\nu$ ES to  $\bar{\nu}$ ES cancels sensitivity to beyond Standard Model physics effects from the NC to CC coupling ratio,  $\rho$ , which are among the primary physics goals of the NuSOnG measurement. In contrast, there is no such cancellation in the ES to IMD ratio.

### 3.4 Beyond Standard Model reach

Elastic neutrino electron scattering is a purely leptonic electroweak process. It can be computed within the Standard Model with high precision [79] and hence provides a very clean probe of physics beyond the Standard Model. The effect of new, heavy ( $M_{\text{new}} \gg \sqrt{s}$ ) degrees of freedom to  $\nu_\mu e^- \rightarrow \nu_\alpha e^-$ , where  $\alpha = e, \mu, \tau$  can be parameterized by the effective Lagrangian

$$\mathcal{L}_{\text{NSI}}^e = + \frac{\sqrt{2}}{\Lambda^2} \left[ \bar{\nu}_\alpha \gamma_\sigma P_L \nu_\mu \right] \left[ \cos \theta \bar{e} \gamma^\sigma P_L e + \sin \theta \bar{e} \gamma^\sigma P_R e \right] \quad (1)$$

New physics, regardless of origin<sup>2</sup>, manifests itself through two coefficients:  $\Lambda$  and  $\theta$ .  $\Lambda$  is the mass scale associated with the new physics, while  $\theta \in [0, 2\pi]$  governs whether the new physics interacts mostly with right-chiral or left-chiral electrons, and also governs whether the new physics contribution interferes constructively or destructively with the Standard Model process ( $Z$ -boson  $t$ -channel exchange) in the case  $\alpha = \mu$ .

Fig. 5 depicts NuSOnG’s ability to exclude  $\Lambda$  as a function of  $\theta$  for  $\alpha = \mu$  or  $\alpha \neq \mu$  assuming its  $\nu - e$  elastic scattering data sample is consistent with Standard Model expectations. It also depicts NuSOnG’s ability to measure  $\Lambda$  and  $\theta$  in case a significant discrepancy is observed. For more details see Ref. [3]. In the case  $\alpha = \mu$ , where new physics effects interfere with the Standard Model contribution, NuSOnG is sensitive to  $\Lambda \lesssim 4$  TeV while in the  $\alpha \neq \mu$  case NuSOnG is sensitive to  $\Lambda \lesssim 1.2$  TeV. The new physics reach of NuSOnG is competitive and also complementary to that of the LHC, where new physics in the neutrino sector is hard to access. The new physics reach of NuSOnG is competitive with other leptonic probes (which involve only charged leptons), including LEP2 [80], and precision measurements of Møller scattering [81].

Several specific new physics scenarios can be probed by a high statistics, high precision measurement of neutrino–matter interactions. NuSOnG’s reach to several heavy new physics scenarios is summarized in Fig. 6. There, we consider not only information obtained from neutrino–electron elastic scattering and inverse muon decay but also from neutrino–quark scattering (both neutral current and charge current). If the new physics scale is below a few TeV, we expect NuSOnG data to significantly deviate from Standard Model expectations.

A more detailed comparison of NuSOnG’s capabilities is summarized in Table 4.

Finally, NuSOnG is also sensitive to the existence of new *light* degrees of freedom, including neutral heavy leptons. A particularly interesting signal to look for is wrong-sign inverse muon decay ( $\bar{\nu}_\mu + e^- \rightarrow$

---

<sup>2</sup>We are neglecting neutrino currents involving right-handed neutrinos or lepton-number violation. These are expected to be severely suppressed as they are intimately connected to neutrino masses (and, to a lesser extent, charged-lepton masses). Once constraints related to neutrino masses are taken into account, these contributions are well outside the reach of TeV-sensitive new physics searches.

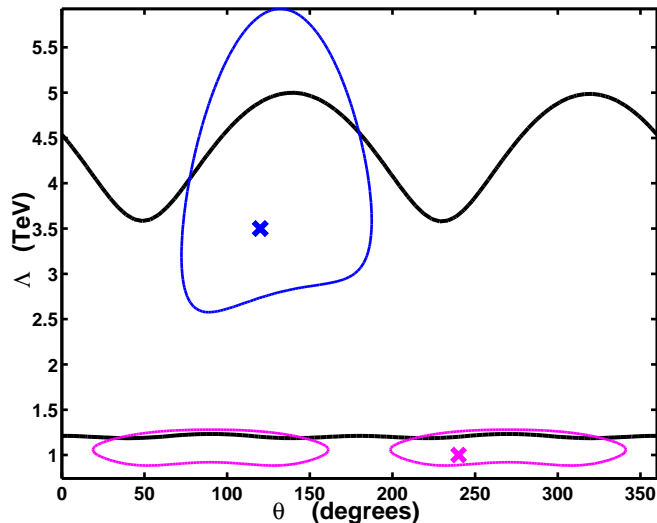


Figure 5: Dark Lines: 95% confidence level sensitivity of NuSONG to new heavy physics described by Eq. (1) when  $\nu_\alpha = \nu_\mu$  (higher curve) and  $\nu_\alpha \neq \nu_\mu$  (lower curve). Closed Contours: NuSONG measurement of  $\Lambda$  and  $\theta$ , at the 95% level, assuming  $\nu_\alpha = \nu_\mu$ ,  $\Lambda = 3.5$  TeV and  $\theta = 2\pi/3$  (higher, solid contour) and  $\nu_\alpha \neq \nu_\mu$ ,  $\Lambda = 1$  TeV and  $\theta = 4\pi/3$  (lower, dashed contour). Note that in the pseudoelastic scattering case ( $\nu_\alpha \neq \nu_\mu$ ),  $\theta$  and  $\pi + \theta$  are physically indistinguishable. From Ref. [3].

Model	Contribution of NuSONG Measurement
Typical $Z'$ Choices: $(B - xL), (q - xu), (d + xu)$	At the level of, and complementary to, LEP II bounds.
Extended Higgs Sector	At the level of, and complementary to, $\tau$ decay bounds.
R-parity Violating SUSY	Sensitivity to masses $\sim 2$ TeV at 95% CL. Improves bounds on slepton couplings by $\sim 30\%$ and on some squark couplings by factors of 3-5.
Intergenerational Leptoquarks (non-degenerate masses)	Accesses unique combinations of couplings. Also accesses coupling combinations explored by $\pi$ decay bounds, at a similar level.

Table 4: Summary of NuSONG's contribution in the case of specific models. See Ref. [3] for details.

$\bar{\nu}_\alpha + \mu^-$ ), which, given our current understanding of neutrino masses and lepton mixing, only occurs at a negligible level. Wrong-sign inverse muon decay would point to short oscillation length neutrino oscillations mediated by sterile neutrinos, a non-unitary lepton mixing matrix, or other non-standard neutrino interactions.

In summary, NuSONG is sensitive to a wide range of beyond Standard Model physics and complementary to new physics which might be observed at the LHC. The program is also complementary to the  $\nu_\tau$  experiment and Neutral Heavy Lepton search described below. This unique physics capability arises from the high-flux, high-energy neutrino beam produced by primary protons at  $\sim 1$  TeV, which allows normalization to IMD events for the first time.

Parallel to the studies summarized in this paper, an independent analysis of high-precision QCD topics possible with a new high-energy neutrino beam was carried out. These high-precision measurements are sensitive to Charge Symmetry Violations and other new physics processes that can significantly influence precision Standard Model parameter extraction. In addition, the large statistics allows the separate extraction of  $n$  and  $n$ -bar structure functions leading to measurements of both  $DxF2$  and  $DxF3$  as well as  $RL$  for  $n$  and  $n$ -bar. Finally, this high statistics QCD study will

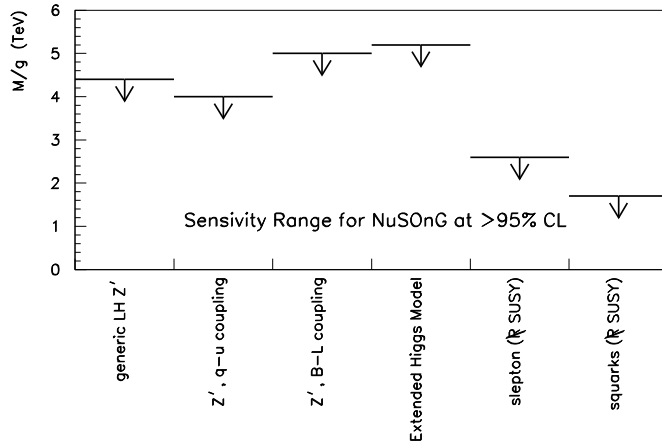


Figure 6: Some examples of NuSOng’s  $2\sigma$  sensitivity to new high-mass particles commonly considered in the literature. For explanation of these ranges, and further examples, see Ref. [3].

include large samples on different nuclear targets allowing us to disentangle the nuclear effects present in neutrino-nucleus processes that appear to be different than the nuclear effects in charged-lepton scattering.

## 4 $\nu_\tau$ Experiments

Since the discovery of the charged  $\tau$  lepton [82], physicists have assumed the existence of a weak partner particle,  $\nu_\tau$ , analogous to the neutrino partners of the  $e$  and  $\mu$  leptons as required by the Standard Model and directly observed for the first time only recently by the DONuT experiment [83, 84]. Indeed, the wealth of studies of charged  $\tau$  lepton properties also require an accompanying tau-neutrino ( $\nu_\tau$ ) for a consistent description of the observed dynamics. Little is directly known about the  $\nu_\tau$  itself<sup>3</sup>. To date, only nine  $\nu_\tau$  charged-current events have ever been detected [83, 84] and all other information we have on this neutrino weak eigenstate is indirect<sup>4</sup>. An experiment sensitive to  $\tau$  leptons placed along the path of an intense,  $\nu_\tau$ -rich neutrino beam would add significantly to our understanding of electroweak interactions and would be sensitive to certain hard-to-get manifestations of new physics.

Advances in the development of Liquid Argon Time Projection Chambers (LArTPCs), notably for the ArgoNeuT [87] and MicroBooNE [88] Fermilab projects and ICARUS-T600 [89] at LNGS, suggest it would be a good choice of base detector technology. A 1 kiloton LArTPC would fulfill the physics requirements to discriminate high energy  $\nu_\tau$  charged current interactions while also providing a useful step in the development of LArTPC technology. Experience with progressively larger LArTPC devices will enable easier deployment for future projects with requirements for fiducial masses of 5 kilotons

<sup>3</sup>We will henceforth mean by “ $\nu_\tau$ ”, the neutrino initially prepared in the weak eigenstate with  $\tau$  lepton number  $\pm 1$ , as the mass and weak eigenstates of the Standard Model neutrinos have been shown to be distinct with the observation of neutrino oscillation.

<sup>4</sup>Solar and atmospheric neutrino experiments have data which is best interpreted as evidence for  $\nu_\tau$  neutral current interactions. The Super-Kamiokande atmospheric neutrino data also statistically favors the presence of both neutral current and charged current  $\nu_\tau$  initiated events [85, 86].

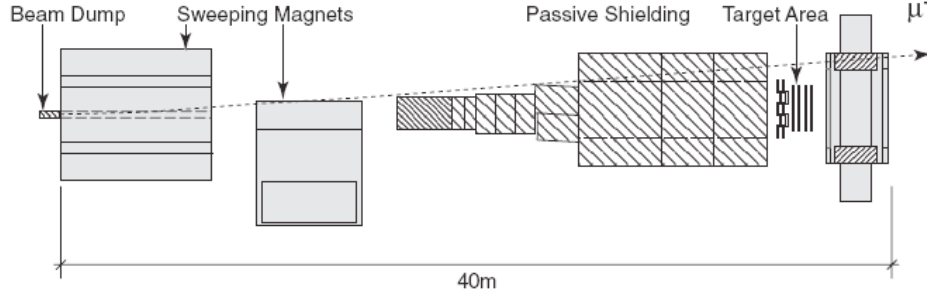


Figure 7: Schematic plan view of the DONuT neutrino beam [83]. The 800 GeV protons are incident on the beam dump from the left. The emulsion modules are located within the target area, 36 m from the beam dump. The trajectory of a 400 GeV/ $c$  negative muon is shown. The proposed LArTPC  $\nu_\tau$  observation experiment will be assumed for this discussion to use a similar neutrino production facility with all detector elements downstream of the passive shielding replaced by a LArTPC.

or more, as has been suggested for future long-baseline neutrino-oscillation experiments at the Deep Underground Science and Engineering Laboratory (DUSEL) [90] and other facilities.

#### 4.1 The neutrino source

For discussion of this  $\nu_\tau$  experiment, we assume a similar neutrino production facility as was used for DONuT [83], as shown in Fig. 7, but at the higher intensity described elsewhere in this document and using a different detector. Neutrinos delivered to the detector are the result of the decay of particles in hadronic showers produced by primary proton interactions. The primary proton beam is expected to be 800 GeV provided by the FNAL Tevatron or CERN SPS+, in which the maximum center-of-mass energy of an incident proton with a nucleon in the target is approximately 40 GeV, well above threshold to produce charm as well as bottom hadrons. Alternatively, if the primary proton beam were produced by a facility such as CERN’s LHC with up to 7 TeV protons in a fixed-target program, the maximum center-of-mass energy rises to approximately 120 GeV, significantly enhancing the  $\nu_\tau$  flux by the decay of produced on-mass-shell  $Z^0$  and  $W^\pm$  bosons to charm hadrons,  $\tau^\pm$ , and  $\nu_\tau$ .

After the interaction of 800 GeV protons with the beam dump,  $\nu_\tau$  are produced primarily by the subsequent decay of produced  $D_s$  mesons, with a branching fraction  $\mathcal{B}(D_s^- \rightarrow \tau^- \bar{\nu}_\tau) = (6.6 \pm 0.6)\%$  [91]. Incident protons are stopped in a beam dump in the form of a tungsten alloy block; DONuT used a 10 cm  $\times$  10 cm  $\times$  1 m water-cooled block. The increased intensity of today’s proton facilities may require optimization of the beam dump. Following the beam dump are dipole magnets sufficient to absorb interaction products and deflect away high energy muons from the beam center. After the magnets, a passive absorber is required to further reduce the flux of muons and other interaction products from the beam center. DONuT used 18 m of steel not more than 2 m from the beam center for this purpose. Emerging from this absorber are a reduced flux of muons and a flux of neutrinos of which 3% will be  $\nu_\tau + \bar{\nu}_\tau$ . The prediction for the spectra of all three neutrino flavors observed at the DONuT emulsion target and using the DONuT beam is shown in Fig. 8. The intensity of the present Tevatron will result in an integrated proton flux approximately 150 times that delivered to DONuT.

#### 4.2 The detector

The requirements for an optimal neutrino detector include (a) large mass, (b) low unit cost, (c) long-term reliable operation, (d) low energy threshold, (e) high spatial resolution, (f) good energy resolution, (g) homogeneous media allowing consistent detection capability throughout, (h) density and radiation

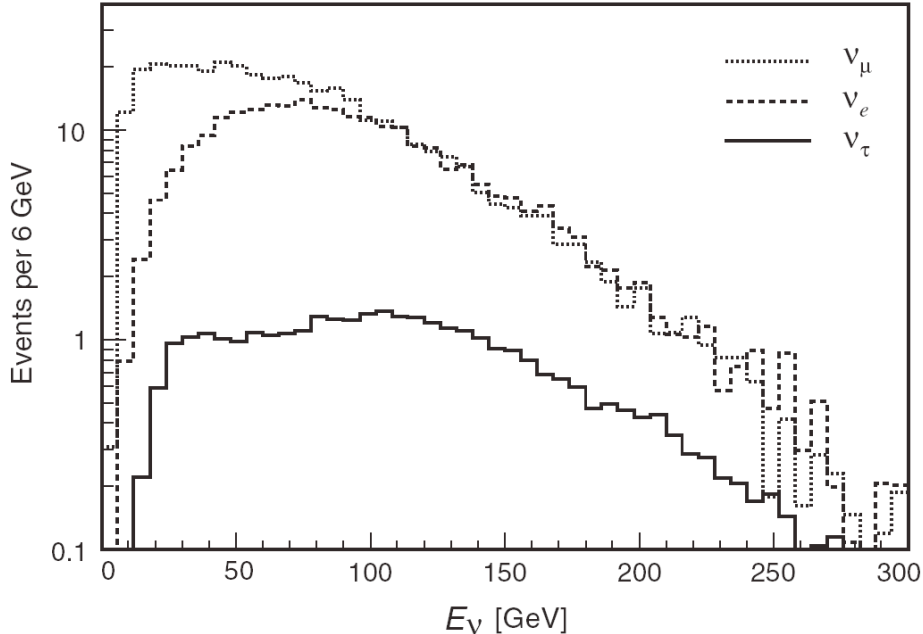


Figure 8: Calculated energy spectra of neutrinos interacting in the DONuT emulsion target [83]. The proposed LArTPC  $\nu_\tau$  observation experiment would see similar spectra at a significantly increased rate.

length balanced between event containment and spatial resolution of electromagnetic showers, and (i) high particle-identification efficiency. The DONuT experiment used a primary detector composed of 260 kg of nuclear emulsion modules stacked along the beam line, with each module exposed only for a limited time to avoid track density higher than  $10^5$  per  $\text{cm}^2$ . With the increased intensity of the expected proton beam and significantly larger event sample required for a precision  $\nu_\tau$  appearance measurement, an emulsion detector is much more difficult. Technologies that may satisfy the above requirements are water Cherenkov detectors, as employed by (*e.g.*) T2K [92], or LArTPCs used by current and developing experiments ArgoNeuT [87], MicroBooNE [88], and ICARUS-T600 [89]. Spatial and energy resolution, low energy threshold, and high-efficiency particle identification are characteristics of LArTPC detectors which will allow the full reconstruction of  $\nu_\tau$  charged-current interactions with efficient identification of the resulting charged  $\tau$ . The use of a LArTPC as the primary detector technology facilitates the identification of typical charged  $\tau$  decay products with excellent vertex and energy reconstruction sufficient to kinematically reconstruct the intermediate  $\tau$ . Although  $\nu_\tau$  events can be identified kinematically, it is interesting to note the possibility of reconstructing the short  $\tau$  track in the highest energy interactions (*i.e.* a 200 GeV  $\tau$  travels a mean distance of 9.7 mm, much larger than the position resolution along the beam direction). With this technology, the energy resolution of hits and reconstructed objects within the detector will allow efficient identification of charged particles (electrons, muons, protons, pions, kaons) as well as  $\pi^0$ 's, all necessary for kinematic reconstruction of charged  $\tau$ 's. Kinematic separation of  $\nu_\tau$  charged current interactions with  $\tau \rightarrow \ell\nu\bar{\nu}$  decays from  $\nu_\mu$  and  $\nu_e$  charged current interactions is possible by analysis of missing transverse momentum, non-zero for  $\nu_\tau$  charged current interactions and close to zero otherwise.

Preliminary scanning of simulated NC and CC  $\nu_e$ ,  $\nu_\mu$ , and  $\nu_\tau$  events up to 300 GeV, based on a MicroBooNE-like LArTPC with 3mm wire spacing, verifies the viability of the technology to meet the physics goals of the proposed experiment. Distinct electromagnetic showers from electrons and photons, tracks from muons, pions, kaons, protons, as well as displaced vertices due to (*e.g.*) pho-

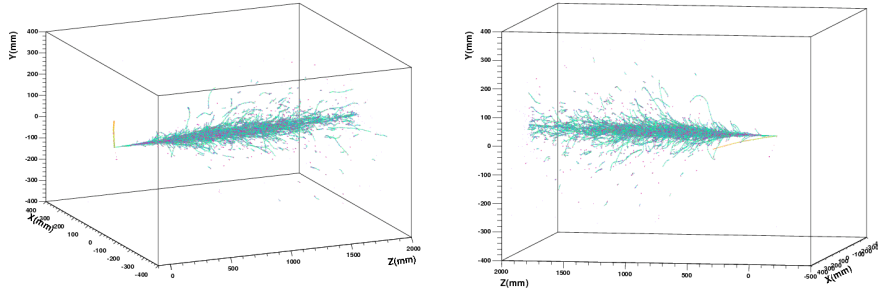


Figure 9: Two arbitrary views of a simulated 193 GeV  $\nu_\tau$  CC interaction in a magnetized MicroBooNE-like LArTPC with 3 mm wire spacing in the charge collection planes. The subsequent 192 GeV  $\tau^-$  promptly decays as  $\tau^- \rightarrow e^- \nu_\tau \bar{\nu}_e$ . The proton from a recoil resonance decay ( $\Delta^{++} \rightarrow p \pi^+$ ) is also clearly visible. The charge drift direction is along the Y-axis. Assumed single hit position resolution is 3 mm in X and Z, 1.5 mm in Y.

ton conversion,  $K_S^0$ , and  $\Lambda^0$ , are clearly evident, facilitating the identification of individual particles and resonances. Example simulated  $\nu_\tau$  CC events are shown in Figs. 9 and 10, demonstrating the expected resolution and pattern of energy deposition hits from typical interactions. This position and calorimetric resolution is absolutely necessary in order to kinematically reconstruct a charged  $\tau$  from its decay products.

The concept of adding a magnetic field to a LArTPC has recently been proposed, with bench tests of its practicality performed on small detectors [93]. This project may offer the first step at deploying the technology at the kiloton scale. If a magnetic field is employed within the TPC, charge-sign identification is possible, which will reduce the combinatorial background in kinematically reconstructing  $\nu_\tau$  charged current interactions, allow separate  $\nu_\tau$  and  $\bar{\nu}_\tau$  measurement, provide a method of observing potential direct  $CPV$  in neutrino and charged  $\tau$  interactions, and provide a second method of track momentum/energy determination especially useful for events with exiting tracks.

One of the major concerns with LArTPC technology is LAr purity, with current technology limiting charge drift distance to less than 2-3 m. The neutrino events at the  $\mathcal{O}(100 \text{ GeV})$  scale will be very forward boosted, such that the LArTPC's drift distance can be short relative to the beam-coordinate. Therefore, sufficient LAr purity may be attained with existing purification technology, even for a kiloton-scale detector, at the expense of additional readout planes or a smaller modular geometry.

Combining the increased flux of protons delivered by the proton source (*e.g.* the FNAL Tevatron) with the use of a LArTPC detector with a mass  $2 \times 10^3$  times that of DONuT's 0.5 ton as well as twice the running time, will result in a delivered flux observed at the detector approximately  $6 \times 10^5$  that observed by DONuT over its six-month run, equivalently  $\mathcal{O}(6 \text{ million})$   $\nu_\tau$  charged current interactions with one year of data.

### 4.3 The Standard Model and beyond

Here we highlight the prospects for measuring charged and neutral current  $\nu_\tau$ -matter scattering, observing  $\nu_\tau$ -electron scattering and probing electromagnetic properties of the tau neutrino. In the Standard Model,  $\nu_\tau$  charged current interactions are mediated by  $W$ -boson exchange. There is only one measurement (with error bars around 50%) of the charged-current scattering cross-section with initial-state tau neutrinos [83], and it agrees with Standard Model expectations. The expectations are that the  $\nu_\tau \rightarrow \tau$  transitions are well-described by the Standard Model thanks to abundant data on  $\tau$

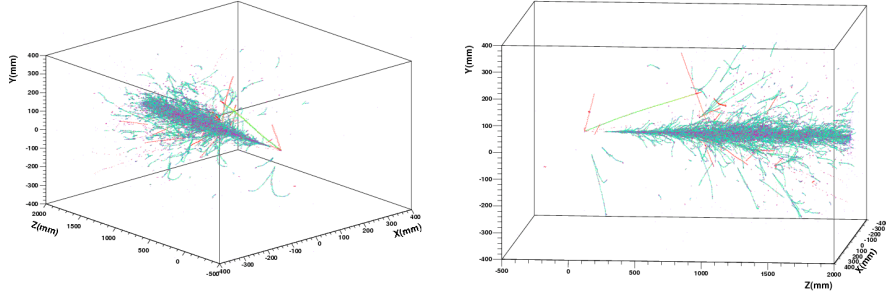


Figure 10: Two arbitrary views of a simulated 220 GeV  $\nu_\tau$  CC interaction in a magnetized MicroBooNE-like LArTPC with 3 mm wire spacing in the charge collection planes. The resulting 212 GeV  $\tau^-$  decays as  $\tau^- \rightarrow \rho^- \nu_\tau$ . The  $\rho^-$  daughter  $\pi^-$  and  $\pi^0$  yield a clear track and electromagnetic shower emanating from the interaction vertex. The products of a recoil resonance decay ( $\Delta^+ \rightarrow p \pi^0$ ) are also evident as a low energy vertex proton track and two low energy displaced-vertex daughter photons. The charge drift direction is along the Y-axis. Assumed single hit position resolution is 3 mm in X and Z, 1.5 mm in Y.

lepton processes, including  $\tau \rightarrow \nu_\tau \ell \nu_\ell$  ( $\ell = e, \mu$ ),  $\tau \rightarrow \nu_\tau + \text{hadrons}$ ,  $D_{(s)} \rightarrow \tau \nu_\tau$ , etc. The measurement precision of  $\nu_\tau$  charged-current events is of the utmost importance as it provides a normalization for neutral-current measurements, which are only very poorly constrained. Furthermore, a  $\tau$ -lepton sensitive neutrino detector may also place bounds on flavor-violating processes such as  $\nu_{e,\mu} + X \rightarrow \tau + Y$ . Even though these are already strongly constrained by the NOMAD experiment [94], a  $\nu_\tau$ -rich beam might significantly improve on current bounds.

In the Standard Model, neutral current interactions are mediated by  $Z$  boson exchange. Unlike charged-current processes, neutral current processes involving  $\nu_\tau$  are only very poorly constrained, especially for interactions with final state  $\nu_\tau$  and  $\nu_e$  [95]. In more detail, if we add to the Standard Model effective operators of the type (see Eq. (1))

$$\mathcal{L}_{\text{NSI}}^{\nu_\tau} = \sum_{f=e,u,d} \frac{\sqrt{2}}{\Lambda^2} \left[ \bar{\nu}_\alpha \gamma_\sigma P_L \nu_\tau \right] \left[ \cos \theta_f \bar{f} \gamma^\sigma P_L f + \sin \theta_f \bar{f} \gamma^\sigma P_R f \right], \quad (2)$$

current data constrain  $\Lambda \lesssim 100$  GeV for all  $f$  and  $\theta_f$  for  $\alpha = e, \tau$ . If present, such weak-scale new physics processes are not only allowed but known to significantly impact the interpretation of neutrino oscillation experiments (see, for example, Ref. [96] for a detailed discussion). A high statistics  $\nu_\tau$ -rich experiment should be able to significantly improve on current bounds or, perhaps, reveal new physics in the neutrino sector.

Finally, a high statistics experiment should also be sensitive to  $\nu_\alpha + e$ -scattering events. These can be used (see section on NuSONG) to look for different manifestations of physics beyond the Standard Model. With a  $\nu_\tau$ -rich beam, one can place bounds on what is usually referred to as the magnetic moment of the tau neutrino. In more detail, one is sensitive to interactions of the type

$$\mathcal{L}_{\text{mag.mom.}} = \frac{\lambda^{\alpha\beta}}{\Lambda} \left[ \bar{\nu}_\alpha \sigma^{\rho\sigma} \nu_\beta \right] F_{\rho\sigma}, \quad (3)$$

where  $\alpha, \beta = e, \mu, \tau$  and  $F_{\rho\sigma}$  is the electromagnetic field-strength. The nature of the dimensionless coefficients  $\lambda$  depends on the nature of the neutrino fields (Majorana versus Dirac) and their magnitude is expected to be negligibly small in the absence of new physics beyond the Standard Model, which

here is characterized by the new physics scale  $\Lambda$ . What is referred to as the magnetic moment of a particular neutrino flavor is process dependent and involves different functions of the  $\lambda$  coefficients. While bounds on the  $\nu_e$  and  $\nu_\mu$  magnetic moments are presently many orders-of-magnitude better than that of  $\nu_\tau$ , it is clear that the information one can acquire with a next-generation  $\nu_\tau$  experiment is independent from and possibly competitive with measurements previous obtained with  $\nu_e$  and  $\nu_\mu$  scattering (even if neutrinos are Majorana fermions and the appropriate matrix of  $\lambda$ -coefficients is anti-symmetric). The proposed  $\nu_\tau$  experiment is wholly complementary to a next-generation program measuring  $\nu_e$  and  $\nu_\mu$  scattering, such as NuSOnG. Astrophysics also provides some stringent flavor-independent bounds, but these are often model dependent and need to be confirmed by terrestrial experiments. Finally, we note that other electromagnetic properties of the tau neutrino can be probed by neutrino electron scattering (see, for example, Ref. [97]).

Additionally, an intense  $\nu_\tau$ -rich neutrino beam offers a potentially large sample of highly polarized single charged  $\tau$  leptons which may be uniquely exploited to measure the charged  $\tau$  anomalous magnetic moment form factor as well as the  $CPV$  electric dipole moment. This sample of neutrino-produced single  $\tau$ 's may also provide an independent measurement of other  $\tau$  properties in an environment with very different systematic uncertainties than those of the electron-positron collider experiments where the vast majority of  $\tau$  physics has been studied in the last three decades.

#### 4.4 Primary measurements

The combination of LArTPC's fast triggering, high spatial and energy resolution, and particle identification by specific ionization energy loss allows a rich program of neutrino physics. The primary measurement of this experiment will be the high precision relative cross section measurement,  $\sigma_\tau/\sigma_{(\mu,e)}$ , for charged current interactions of  $\nu_e$ ,  $\nu_\mu$ , and  $\nu_\tau$  neutrinos, which provides a sensitive test of the Standard Model as outlined in the previous section. When combined with measurements/limits from NuSOnG or current limits on the magnetic moment of  $\nu_\mu$  and  $\nu_e$ , similar searches for events consistent with neutrino magnetic moment interactions in a  $\nu_\tau$ -rich beam can provide sensitivity to the  $\nu_\tau$  magnetic moment comparable to the present limits for  $\nu_e$  and  $\nu_\mu$ .

Despite the much smaller sample of  $\tau$ 's as compared to present B-factories ( $\mathcal{O}(10^9)$   $\tau$ 's), the unique environment of this detector and production mechanism provide a very different set of systematic uncertainties which allow an interesting laboratory for the verification of virtually all  $\tau$  properties, including branching fraction measurements as small as  $\mathcal{O}(10^{-5})$ . For example, utilizing the sample of  $\mathcal{O}(10^6)$  charged  $\tau$  leptons resulting from  $\nu_\tau$  charged current interactions with one year of exposure, several measurements of charged  $\tau$  properties are also possible. In particular, due to the significant and predictable polarization of the single charged  $\tau$ 's produced by  $\nu_\tau$  charged current interactions, this experiment is potentially much more sensitive to the anomalous magnetic moment form factor and electric dipole moment of the charged  $\tau$  than previous experiments.

Further neutrino physics which may be measurable in this detector includes exclusive cross section measurements, such as coherent-pion production in neutral current and charged current interactions as well as  $\nu_\tau e$  charged and neutral current interactions. The significant size and low energy threshold of the LArTPC also allows measurement of solar neutrino rates as well as burst-supernova neutrino sensitivity out of time with the beam spill. The proximity of the detector to the surface, expected pointing resolution of reconstructed tracks, and the size of the detector will yield a significant rate of cosmic-ray induced muons offering a wealth of interesting potential opportunities ranging from the observation of climactic changes in the atmosphere to searching for point sources of cosmic rays and sensitivity to the solar magnetic field.

## 4.5 $\nu_\tau$ summary

Though the  $\nu_\tau$  has been assumed to exist for over thirty years, only nine  $\nu_\tau$  charged current interactions have been observed directly. Precision study of this particle and its interactions is clearly warranted in order to determine if its nature is as predicted by the Standard Model and provides a unique laboratory to search for new physics. The proposed program of neutrino and charged  $\tau$  physics is broad enough to support a wide variety of studies alongside the primary studies of the electroweak interactions of the  $\nu_\tau$  using  $\mathcal{O}(10^5)$  larger sample of interactions than has been observed previously. The proposed 1 kt size of the LArTPC for this experiment is a natural choice to achieve the desired physics goals while also providing an intermediate step in the development of the LArTPC technology between MicroBooNE (100 t) and DUSEL (5+ kt). The addition of a solenoidal field would significantly enhance the physics capabilities of the project while pioneering the technological advancement of coupling LArTPCs with a magnetic field at the kiloton scale.

## 5 Searches for Exotic Neutrinos

Singlet (sterile) neutrino states arise in models which try to implement massive (light) neutrinos in extensions of the Standard Model. Three singlet states  $N_1$ ,  $N_2$  and  $N_3$  are associated with the three active neutrinos. In the original see-saw mechanism, these new states have very large masses, but variations like the nMSM model [98] give them masses which are within reach of experimental searches. Limits exist from laboratory experiments, but they extend to masses up to 450 MeV, and apply to couplings with the  $\nu_e$  or  $\nu_\mu$ . An upgraded Tevatron machine could enlarge the domain of exploration in masses and couplings with the study of neutrinos coming from  $D$  and  $B$  decays. For the first time, mixings to the  $\nu_\tau$  could be efficiently investigated. Such a search can be envisaged in the beam-dump of the  $\nu_\tau$  experiment.

### 5.1 Production of sterile neutrinos

If heavy neutrinos exist, they mix with active neutrinos through a unitary transformation. Any neutrino beam will contain a fraction of heavy neutrinos at the level  $U_{Nl}^2$  where  $U$  denotes the mixing matrix element between the heavy state  $N$  and the charged lepton,  $l$  ( $l$  being  $e$  or  $\mu$  or  $\tau$ ). At low energy accelerators, neutrinos are produced in  $\pi$  and  $K$  decays. At higher energies, charm and beauty contribute. Kinematically, the mass range allowed for the production of a heavy  $N$  depends on the emission process. In  $\pi \rightarrow \mu + N$  decays, sterile neutrinos can reach a mass of 30 MeV. In  $\pi \rightarrow e + N$  channels, the range increases to 130 MeV. Kaons allow larger masses, up to 450 MeV.  $D$  decays extend the range to  $\sim 1.4$  GeV for  $e$  and  $\mu$  channels, (but only to 180 MeV for the  $\tau$  channel), and  $B$  decays to  $\sim 4.5$  GeV (3 GeV for the  $\tau$  channel). The flux of  $N$  accompanies the flux of known neutrinos at the level of  $U_{Nl}^2$ . Corrections to this straightforward result come from helicity conservation which applies differently here. For example, for massless neutrinos, it suppresses  $\pi \rightarrow e + \nu$  decays relative to  $\pi \rightarrow \mu + \nu$  decays. This is not true anymore for  $\pi \rightarrow e + N$ . Phase space considerations have also to be taken into account. Thus, precise calculations have to be done in all possible cases to be considered. For example, precise branching fractions in the case of massive neutrinos have been calculated in Ref. [99].

### 5.2 Decays of sterile neutrinos

$N$ 's are not stable. They will decay through purely weak interactions. The lifetime critically depends on the mass considered; it varies as  $m^5$  power. Decay modes also depend on the  $N$  mass. As soon as the mass is greater than 1 MeV, the first channel to open is  $N \rightarrow ee\nu$ . With increasing masses, new modes open, and one can obtain  $e\mu\nu$ ,  $\pi e$ ,  $\mu\mu\nu$ ,  $\pi\mu$ . For higher mass states potentially produced in

$B$  decays, new modes become relevant. For example, for masses above 2 GeV, one can envisage the channels  $De$ ,  $D\mu$  or even  $D\tau$ . Exact branching fractions require precise calculations. The lifetime is given by the formula applying to weak decays, apart from a general suppression factor coming again from the mixing  $U_{Ni}^2$ . Other factors coming from helicity and phase space considerations have to be included.

### 5.3 Previous results

The search consists in looking for a decay signature, typically two charged tracks, one of them being a lepton, and reconstructing a vertex in an empty volume. If no candidates are found, one sets a limit in a two-dimensional plane, mass vs. mixings. Mixings can be equal or different in production and decay. Thus, one tests 6 different combinations of mixings in principle. This has been attempted at CERN by the low energy experiment PS191 [100] with  $5 \times 10^{18}$  protons of 19 GeV on target, or about  $10^{15}$  neutrinos (essentially all  $\nu_\mu$ ) crossing an empty detector volume. The neutrinos were produced in  $\pi$  and  $K$  decays. Thus the limits apply to couplings to  $\nu_e$  and  $\nu_\mu$ . Kinematically, the  $\tau$  is not accessible either in production or in decay. The explored mass range is limited to the  $K$  mass. The limits on the  $U_{Ni}^2$  couplings reach the level of  $10^{-8}$  in a large range of accessible masses and for all combinations of mixings to  $e$  or  $\mu$ . Soon-to-run experiments (such as MINERvA [101]) could improve these results by an order of magnitude. In order to increase the domain of exploration, it is necessary to consider higher energy beams producing neutrinos via  $D$  and  $B$  decays.  $D_s$  decays into  $\tau\nu_\tau$ , with a branching fraction of 6%.  $B_s$  decay into the 3 leptonic channels,  $Xe\nu_e$ ,  $X\mu\nu_\mu$ ,  $X\tau\nu_\tau$ , with branching fractions 10%, 10% and 5%, respectively. This allows the search of  $N$  states with masses up to 4.5 GeV, mixing in particular with the  $\nu_\tau$ . Since the limits vary as the square root of the accumulated neutrino flux, the number of protons on target has to be maximal.

### 5.4 Detector considerations

The experiment consists in detecting a decay vertex arising in an empty volume set in a neutrino beam and characterized by, in most cases, two charged tracks. The detector requires a decay volume as large as possible followed by a calorimeter. In principle, the search is better done at low energy. However, in order to extend the region of potential masses, one has to produce  $B_s$  and this is only done at high energy. The advantage of an upgraded Tevatron machine comes directly from the much increased luminosity available. If, instead of being done in a beam dump, the search is done in a neutrino beam, for example in parallel with NuSONG, the background coming from neutrino interactions is also substantially increased. In 12 m of air the number of interactions amounts to several 10000 events. Charged current events will give a muon in the final state in 99% of the cases. It becomes essential to have an evacuated volume with a calorimeter to be able to efficiently identify electrons and muons. Studies have been made for the decay volume. A 12 m long pipe where the vacuum can be pushed down to  $10^{-3}$  atm can be seen in Fig. 11. The background from interactions becomes manageable. A higher vacuum would require much more sophisticated techniques. A good spatial resolution plane is necessary between the decay volume and the calorimeter in order to precisely reconstruct the decay vertex. The best limits on couplings come from exclusive channels:  $\pi e$  and  $\pi\mu$  for low masses,  $Ke$  and  $K\mu$  for intermediate masses, and  $De$ ,  $D\mu$ ,  $\pi\tau$  and  $D\tau$  for higher masses. The decay channels involving  $e$  and  $\mu$  can be totally reconstructed. Two essential constraints arise: 1) the reconstructed direction of arrival must point to the neutrino production target and 2) the invariant mass of the detected particles must reconstruct a fixed mass. For example, one can search for a  $D + e \rightarrow K + \pi + \pi + e$ . This means that the calorimeter must have the track reconstruction and identification capability. It must be fine grained and preferably come with a magnetic field. These constraints are not applicable for decay modes involving a  $\tau$  lepton where a characteristic  $\pi\tau$  will show up.

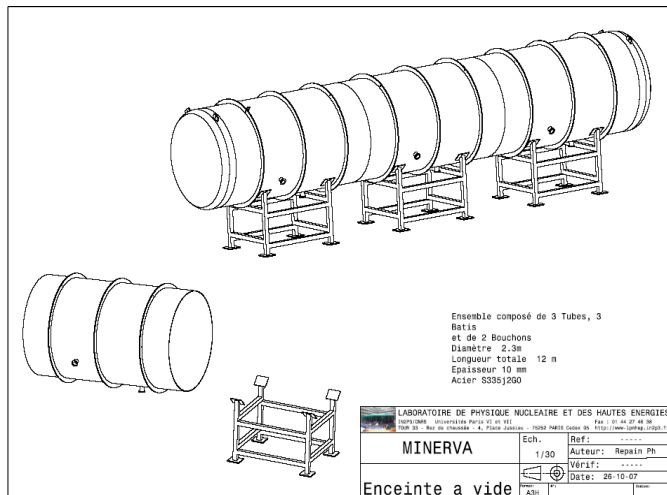


Figure 11: A 12 m long tank for the evacuated decay volume.

## 5.5 Expectations

Extrapolating the neutrino fluxes used in the  $\nu_\tau$  experiment, one expects about  $10^{16}$   $\nu_\tau$  per year traversing a  $3 \text{ m}^2$  section with average energy of 50 GeV. These neutrinos come from  $D_s$  decays. Other  $D$ s give about 20 times more  $\nu_e$  and  $\nu_\mu$ . With a ratio of production cross-sections  $B/D \sim 10^{-3}$  one expects of the order of  $10^{14}$  neutrinos of each type coming from  $B$ s. With these numbers, one can estimate the limits obtained by a null experiment in a 10 m long decay volume.

- From  $D$  decays one reaches a  $U^2$  limit of  $10^{-9}$  for a mass around 1 GeV and mixings to  $e$  and  $\mu$ .
- From  $B$  decays one can reach  $10^{-8}$  for all mixings, in particular the never explored  $U_{\tau\tau}^2$  around a mass of 3 GeV.

Heavy neutral leptons arise in models which try to accommodate massive active neutrinos. Searches have been done in low energy neutrino beams. The advantage of an upgraded high energy machine is two-fold: the high energy allows exploration in a larger domain of masses, up to the  $B$  mass, and the high luminosity pushes down the limits. In particular, it can set meaningful limits on the practically unexplored couplings to the  $\tau$ . The fascinating possibility of finding sterile neutrinos could be uniquely tested in such an experiment.

## 6 Conclusion

This paper presents examples of the compelling physics that can result from a  $\sim 1$  TeV fixed target facility. We have especially highlighted the discovery potential in the charm sector, which would utilize slow-spill beams. We also considered forefront physics in the neutrino sector. We reviewed an existing idea for precision electroweak studies. Also, we presented two new promising and unique avenues for beyond standard model neutrino searches using beam dump production. The first of these uses  $\nu_\tau$  charged current events which are produced above threshold by a proton beam in the 800 GeV to 1 TeV range. The second is a search for neutral heavy leptons produced in the beam dump.

This combination of experiments represents an integrated program aimed at discovery of new physics which is complementary to other approaches under discussion for the future.

## A Specifics of Running 1 TeV Beams: The Tevatron

Previous 800 GeV fixed-target operation of the Tevatron ran with a maximum throughput of roughly  $25\text{-}28 \times 10^{12}$  protons (25-28 Tp) per pulse every 60 sec with a duty cycle of roughly 33-40%. The beam was shared, over a 20-23 sec flat-top period, between slow spill experiments and neutrino experiments which required fast extracted beams. To meet the demands of NuSO<sub>n</sub>G, the facility needs to be able to deliver approximately  $2 \times 10^{20}$  protons on target over five years of running at 66% overall operation efficiency per year. This translates to an average particle delivery rate during running of about 1.8 Tp/sec. Assuming that only a 40 sec ramp will be required for NuSO<sub>n</sub>G, each ramping of the Tevatron would need to deliver about 75 Tp, more than 2.5 times the previous record intensity. The subsections below address some of the major issues regarding re-institution of a Tevatron fixed-target program, and issues associated with meeting the above intensity demand.

### A.1 Magnet ramping

The original Tevatron fixed-target program ran at 800 GeV and stress and strain on the superconducting magnets was a major issue early in the program. Issues with lead restraints within the cryostat were eventually identified and all dipole magnets were repaired in the tunnel in the late 1980's. Since that time, the Tevatron has been able to average over 250,000 cycles between failures of dipole magnets [102]. This “rate” includes failures of collider-specific magnets, such as low-beta quadrupoles. Note that a neutrino program which demands  $2 \times 10^{20}$  POT, using a synchrotron that delivers 75 Tp every cycle, requires about 2.7 million cycles – thus, on the order of 10 failures could be expected during the course of the experiment.

Once the fixed-target operation was halted and only collider operation was foreseen, the capability to repair and rebuild Tevatron magnets was greatly reduced at the laboratory. However, assuming no need for building new magnets from scratch, capabilities still exist to perform repairs and, along with the given inventory of spare Tevatron magnets and corrector packages, a multi-year fixed-target operation consistent with the above is sustainable from this aspect [103].

Ramp rate studies of Tevatron dipole magnets have been performed, and rates of 200-300 A/sec can be maintained at 4.6° K without quenching [104]. The current power supply system can still perform at this level. To increase reliability, however, some PS system components may need to be upgraded. Additionally, the Tevatron RF system is still capable of running in the fixed-target state, though beam loading effects and appropriate compensation will need to be investigated for the anticipated higher intensity operation. Two Main Injector (MI) pulses would be used to fill the Tevatron. At 3 sec per 150 GeV MI cycle, this constitutes a 15% impact on other MI demands.

### A.2 Comments on high intensity

The record intensity extracted from the Tevatron in a cycle at 800 GeV was almost 30 Tp in 1997, though 20-25 Tp was far more typical. At that time, the bunch length during acceleration would shrink to the point where a longitudinal instability at higher energies ( $\sim 600$  GeV), resulting in aborts and sometimes quenches. This was compensated as well as possible with “bunch spreading” techniques (blowing up the emittance via RF noise sources). Today, the Main Injector is capable of providing greater than 40 Tp per pulse, which could, in principle, fill the Tevatron to 80 Tp. Many improvements to the Tevatron beam impedance have been made during Run II, including, for example, reduction of the Lambertson magnet transverse impedances which were identified as major sources. Additionally, advances in RF techniques/technology and damper systems, *etc.*, may allow, with enough studies and money, much better compensation of these effects, if required. This is a primary R&D point, if intensities near 75 Tp are to be realized in the Tevatron.

### A.3 Re-commissioning of extraction system

Returning the Tevatron to fixed-target operation would require the re-installation of the extraction channel in the A0 straight-section from which beam would be transported to the existing Switchyard area and on to the experimental target station. The electrostatic septa were located at the D0 straight section and could straightforwardly be reinstalled in the original configuration. All of this equipment is currently in storage and available for use. The B0 straight section, currently housing the CDF detector, would be replaced with standard long straight section optical components. Thus, the higher heat leak elements presently installed in the B0 and D0 regions would be absent, requiring less demands from the cryogenics system.

The other necessary piece of hardware is the slow-spill feedback system, referred to as “QXR” which employs fast air-core quadrupoles installed at warm straight sections in the Tevatron for fast feedback tune adjustment during the resonant extraction process. Again, this equipment mostly still exists, though it may be desirable to perform a low-cost upgrade to modernize some electronic components.

The neutrino experiment being discussed has requested “pinged” beam, short bursts of particles brought about by the QXR system. NuSOnG will likely require tens of *pings* per cycle, during an assumed 1 sec flat-top. Resonant extraction is an inherently lossy process, on the scale of 1-2%, determined by the particle step size across the thin electrostatic septum wires. Historically, loss rates were tolerable with between 20-30 Tp extracted over 20 sec. Pings, each lasting on the scale of 1-2 ms with approximately 5 Tp per ping – and sometimes higher – were extracted routinely for the Tevatron neutrino program. Thus, 15 or more such pings over a 1 sec flat top should be straightforward. Alternative methods for fast extraction could be contemplated, though perhaps at a price. For instance, if an appropriate RF bunching scheme (using a 2.5 MHz RF system, for example) can be employed to prepare bunches spaced by 400 ns, then a fast kicker magnet system might be able to extract 50 such bunches one-by-one to the Switchyard, a much cleaner extraction process. Spreading the beam across fewer, longer bunches may also help to mitigate coherent instability issues. This opens up another possible R&D point to pursue. To set the scale, the highest intensity extracted in a single pulse (*i.e.* not during a slow spill) without quenching the Tevatron was about 10 Tp [102]. (Also, this was a test, not a normal operational procedure.)

The exact method used for 800 GeV operation would be a point closely negotiated between the laboratory and the experiment(s) using the beam. Both resonant extraction and kicker methods should be feasible within reasonable constraints.

### A.4 Tevatron abort system

The abort system used during high intensity fixed-target operation was located at C0 and was capable of absorbing 1 TeV proton beams at 30 Tp, repeatedly every “several” seconds, to the abort dump. While not used in collider operation, this beam dump and beam delivery equipment near the C0 straight section is still available and still accessible, and requires re-installation of extraction devices and their power supplies. The ultimate parameters of the neutrino experiment being discussed pushes the beam stored energy from about 3.5 MJ (27 Tp at 800 GeV) toward 10 MJ. The design limits of this system would need to be re-examined, and the implications and environmental impact of re-establishing this area as the primary abort must be looked at carefully.

## Acknowledgments

We gratefully acknowledge support from the Department of Energy, the National Science Foundation, the Consejo Nacional de Ciencia y Tecnología and the Universities Research Association (URA) Visiting Scholars at Fermilab Award.

## References

- [1] R. Garoby *et al.*, “Scenarios for Upgrading the LHC Injectors”, CERN-AB-2007-007 (2006).
- [2] R. Garoby, “Upgrade Issues for the CERN Accelerator Complex”, Proc. of EPAC08, Genoa, Italy (2008).
- [3] T. Adams *et al.* (NuSOnG Collaboration), Int. J. Mod. Phys. A **24**, 671 (2009).
- [4] T. Adams *et al.* (NuSOnG Collaboration), “QCD Precision Measurements and Structure Function Extraction at a High Statistics, High Energy Neutrino Scattering Experiment: NuSOnG”, to be submitted to Int. J. Mod. Phys. A.
- [5] J. A. Appel (Ed.), C. N. Brown (Ed.), P. S. Cooper (Ed.), H. B. White (Ed.), *Symposium in Celebration of the fixed-target program with the Tevatron*, FERMILAB-CONF-01-386 (2000) arXiv:0008076 [hep-ex].
- [6] A. Schwartz, Nucl. Phys. B **187**, 224 (2009).
- [7] I. Bigi *et al.*, arXiv:0904.1545 [hep-ph] (2009).
- [8] Y. Grossman, Y. Nir, G. Perez, arXiv:0904.0305 [hep-ph] (2009).
- [9] E. Golowich *et al.*, arXiv:0903.2830 [hep-ph] (2009).
- [10] K. Blum, Y. Grossman, Y. Nir, G. Perez, arXiv:0903.2118 [hep-ph] (2009).
- [11] X. Li and Z. Wei, Phys. Lett B **651**, 330 (2007).
- [12] P. Ball, J. Phys. G **34**, 2199 (2007).
- [13] M. Blanke *et al.*, Phys. Lett. B **657**, 81 (2007).
- [14] Y. Nir, JHEP **0705**, 102 (2007).
- [15] E. M. Aitala *et al.* (E791 Collaboration), Phys. Rev. D **57**, 13 (1998).
- [16] J. M. Link *et al.* (FOCUS Collaboration), Phys. Lett. B **618**, 23 (2005).
- [17] B. Aubert *et al.* (BaBar Collaboration), Phys. Rev. Lett. **98**, 211802 (2007).
- [18] M. Staric *et al.* (Belle Collaboration), Phys. Rev. Lett. **98**, 211803 (2007).
- [19] T. Aaltonen *et al.* (CDF Collaboration), Phys. Rev. Lett. **100**, 121802 (2008).
- [20] I. Abt *et al.* (HERA-B Collaboration), Eur. Phys. Jour. C **52**, 531 (2007) .
- [21] C. Amsler *et al.* (Particle Data Group), Phys. Lett. B **667**, 1 (2008).
- [22] L. Zhang *et al.* (Belle Collaboration), Phys. Rev. Lett. **96**, 151801 (2006).
- [23] <http://superb.kek.jp/>
- [24] <http://www.pi.infn.it/SuperB/>
- [25] P. Spradlin, G. Wilkinson, F. Xing *et al.*, LHCb public note LHCb-2007-049 (2007).
- [26] [http://www.slac.stanford.edu/xorg/hfag/charm/FPCP08/results\\_mix+cpv.html](http://www.slac.stanford.edu/xorg/hfag/charm/FPCP08/results_mix+cpv.html)

- [27] E. Barbiero *et al.* (Heavy Flavor Averaging Group), arXiv:0808.1297 [hep-ex] (2008).
- [28] S. Dobbs *et al.* (CLEOc Collaboration), Phys. Rev. D **76**, 112001 (2007).
- [29] J. M. Link *et al.* (FOCUS Collaboration), Phys. Rev. Lett. **88**, 041602 (2002); Err., Phys. Rev. Lett. **88**, 159903 (2002).
- [30] E. M. Aitala *et al.* (E791 Collaboration), Phys. Lett. B **403**, 377 (1997).
- [31] P. Rubin *et al.* (CLEOc Collaboration), Phys. Rev. D **78**, 072003 (2008).
- [32] B. Aubert *et al.* (BaBar Collaboration), Phys. Rev. D **71**, 091101 (2005).
- [33] J. M. Link *et al.* (FOCUS Collaboration), Phys. Lett. B **491**, 232 (2000); Err., Phys. Lett. B **495**, 443 (2000).
- [34] P. L. Frabetti *et al.* (E687 Collaboration), Phys. Rev. D **50**, 2953 (1994).
- [35] J. M. Link *et al.* (FOCUS Collaboration), Phys. Lett. B **622**, 239 (2005).
- [36] M. Staric *et al.* (Belle Collaboration), Phys. Lett. B **670**, 190 (2008).
- [37] B. Aubert *et al.* (BaBar Collaboration), Phys. Rev. Lett. **100**, 061803 (2008).
- [38] D. Acosta *et al.* (CDF Collaboration), Phys. Rev. Lett. **94**, 122001 (2005).
- [39] S. E. Csorna *et al.* (CLEO Collaboration), Phys. Rev. D **65**, 092001 (2002).
- [40] E. M. Aitala *et al.* (E791 Collaboration), Phys. Lett. B **421**, 405 (1998).
- [41] G. Bonvicini *et al.* (CLEO Collaboration), Phys. Rev. D **63**, 071101 (2001).
- [42] J. E. Bartelt *et al.* (CLEO Collaboration), Phys. Rev. D **52**, 4860 (1995).
- [43] B. Aubert *et al.* (BaBar Collaboration), Phys. Rev. D **78**, 051102 (2008).
- [44] K. Arinstein *et al.* (Belle Collaboration), Phys. Lett. B **662**, 102 (2008).
- [45] D. Cronin-Hennessy *et al.* (CLEO Collaboration), Phys. Rev. D **72**, 031102 (2005).
- [46] S. Kopp *et al.* (CLEO Collaboration), Phys. Rev. D **63**, 092001 (2001).
- [47] X. C. Tian *et al.* (Belle Collaboration), Phys. Rev. Lett. **95**, 231801 (2005).
- [48] G. Brandenburg *et al.* (CLEO Collaboration), Phys. Rev. Lett. **87**, 071802 (2001).
- [49] D. M. Asner *et al.* (CLEO Collaboration), Phys. Rev. D **70**, 091101 (2004).
- [50] G.J. Gounaris and J. J. Sakurai, Phys. Rev. Lett. **21**, 244 (1968).
- [51] S. M. Flatté, Phys. Lett. **63B**, 224 (1976).
- [52] E.P. Wigner, Phys. Rev. **70**, 15 (1946).
- [53] E.P. Wigner and L. Eisenbud, Phys. Rev. **72**, 29 (1947).
- [54] I. J. R. Aitchison, Nucl. Phys. A **189**, 417 (1972).
- [55] C. Zemach, Phys. Rev. **133**, B1201 (1964).

- [56] S. Kopp *et al.* (CLEO Collaboration), Phys. Rev. D **63**, 092001 (2001).
- [57] Y. P. Lau, Ph.D. thesis, Princeton University, 2006 (unpublished).
- [58] S. Spanier, N.A. Tornqvist and C. Amsler, “Note on Scalar Mesons,” in C. Amsler *et al.* (Particle Data Group), Phys. Lett. B **667**, 1 (2008).
- [59] C. Amsler and A. Masoni, “The  $\eta(1405)$ ,  $\eta(1475)$ ,  $f_1(1420)$ , and  $f_1(1510)$ ,” in C. Amsler *et al.* (Particle Data Group), Phys. Lett. B **667**, 1 (2008).
- [60] M. Mattson *et al.* (SELEX Collaboration), Phys. Rev. Lett. **89**, 112001 (2002).  
A. Ocherashvili *et al.* (SELEX Collaboration), Phys. Lett. B **628**, 18 (2005).
- [61] J. Adelman *et al.* (CDF Collaboration), Nucl. Instrum. Meth. A **572**, 361 (2007).
- [62] The NuSONG Expression of Interest is available from the Fermilab Directorate or at <http://www-nusong.fnal.gov>.
- [63] R. Bernstein *et al.*, “Sign-Selected Quadrupole Train”, FERMILAB-TM-1884 (1994). J. Yu *et al.*, “NuTeV SSQT Performance”, FERMILAB-TM-2040 (1998).
- [64] W. G. Seligman *et al.* (CCFR Collaboration) Phys. Rev. Lett **79**, 1213 (1997).  
U. K. Yang *et al.* (CCFR Collaboration) Phys. Rev. Lett **86** 2742 (2001).
- [65] M. Tzanov *et al.* (NuTeV Collaboration), Phys. Rev. D **74**, 012008 (2006).
- [66] J. P. Berge *et al.*, Z. Phys. C **49**, 187 (1991).
- [67] P. Vilain *et al.*, Phys. Lett. B **335**, 246 (1994).
- [68] Q. Wu *et al.* (NOMAD Collaboration), Phys. Lett. B **660**, 19 (2008).
- [69] E. Eskut *et al.* (CHORUS Collaboration), Nucl. Phys. B **793**, 3 (2007).
- [70] C. W. Walter (Super-K Collaboration), Nucl. Instrum. Meth. A **503**, 110 (2003).
- [71] M. H. Ahn *et al.* (K2K Collaboration), Phys. Rev. D **74**, 072003 (2006).
- [72] P. Adamson *et al.* (MINOS Collaboration), Phys. Rev. Lett. **101**, 221804 (2008).
- [73] B. Aharnim *et al.* (SNO Collaboration), Phys. Rev. C **75**, 045502 (2007).
- [74] B. Achkar *et al.*, Phys. Lett. B **374**, 243 (1996).
- [75] M. Apollonio *et al.* (CHOOZ Collaboration), Phys. Lett. B **466**, 415 (1999).
- [76] Z. Daraktchieva *et al.* (MUNU Collaboration), Phys. Lett. B **615**, 153 (2005).
- [77] C. A. Gagliardi, R. E. Tribble and N. J. Williams, Phys. Rev. D **72**, 073002 (2005).
- [78] L. A. Ahrens *et al.*, Phys. Rev. D **41**, 3297 (1990).
- [79] G. 't Hooft, Phys. Lett. B **37**, 195 (1971).
- [80] M. S. Carena *et al.*, Phys. Rev. D **70**, 093009 (2004).
- [81] P. L. Anthony *et al.* (SLAC E158 Collaboration), Phys. Rev. Lett. **95**, 081601 (2005).

- [82] M. L. Perl *et al.*, Phys. Rev. Lett. **35**, 1489 (1975).
- [83] K. Kodama *et al.*, Phys. Rev. D **78**, 052002 (2008).
- [84] K. Kodama *et al.* (DONUT Collaboration), Phys. Lett. B **504**, 218 (2001).
- [85] K. Abe *et al.* (Super-Kamiokande Collaboration), Phys. Rev. Lett. **97**, 171801 (2006).
- [86] S. Fukuda *et al.* (Super-Kamiokande Collaboration), Phys. Rev. Lett. **85**, 3999 (2000).
- [87] ArgoNeuT homepage: <http://t962.fnal.gov>.
- [88] MicroBooNE collaboration, “A Proposal for a New Experiment Using the Booster and NuMI Neutrino Beamlines: MicroBooNE” (2007).
- [89] S. Amerio *et al.* (ICARUS Collaboration), Nucl. Instrum. Meth. A **527**, 329 (2004).
- [90] DUSEL homepage: <http://www.lbl.gov/nsd/homestake>.
- [91] C. AMSLER *et al.* (Particle Data Group), Phys. Lett. B **667**, 1 (2008).
- [92] Y. Itow *et al.* (The T2K Collaboration), arXiv:0106019 [hep-ex] (2001).
- [93] A. Badertscher, M. Laffranchi, A. Meregaglia and A. Rubbia, New J. Phys. **7**, 63 (2005).  
A. Badertscher, M. Laffranchi, A. Meregaglia, A. Muller and A. Rubbia, Nucl. Instrum. Meth. A **555**, 294 (2005). A. Ereditato and A. Rubbia, Nucl. Phys. Proc. Suppl. **155**, 233 (2006).
- [94] P. Astier *et al.* (NOMAD Collaboration), Nucl. Phys. B **611**, 3 (2001).
- [95] S. Davidson, C. Pena-Garay, N. Rius and A. Santamaria, JHEP **0303**, 011 (2003).
- [96] A. Friedland and C. Lunardini, Phys. Rev. D **72**, 053009 (2005).
- [97] M. Hirsch, E. Nardi and D. Restrepo, Phys. Rev. D **67**, 033005 (2003).
- [98] T. Asaka and M. Shaposhnikov, Phys. Lett. B **620**, 17 (2005). M. Shaposhnikov, Nucl. Phys. B **763**, 49 (2007). M. Shaposhnikov, “Dark Matter: The Case of Sterile Neutrino”, Proc. of Berlin 2006: Marcel Grossmann Meeting on General Relativity, Berlin, Germany (2007). A. D. Dolgov *et al.*, Nucl. Phys. B **590**, 562 (2000). M. Viel *et al.*, Phys. Rev. D **71**, 063534 (2005).
- [99] J. M. Levy, Ph.D. thesis, University of Paris, 1986 (unpublished).
- [100] G. Bernardi *et al.*, Phys. Lett. B **166**, 479 (1986).
- [101] D. Drakoulakos *et al.* (Minerva Collaboration), arXiv:0405002 [hep-ex] (2004).
- [102] G. Annala, private communication.
- [103] D. Harding, Fermilab internal memo, 26 March 2008 (unpublished).
- [104] A. Mokhtarani, “Results of Tevatron Dipole Tests at 3.6 K”, MTF-93-0010 (1993).